

Finite Element Analysis and Mathematical Modeling of a Novel Magnetorheological Honing Process

A Dissertation Submitted

In Partial Fulfillment of the Requirements
for the Degree of

Master of Engineering
in
CAD/CAM and Robotics
by

Vishwas Grover



to the

**MECHANICAL ENGINEERING DEPARTMENT
THAPAR UNIVERSITY, PATIALA**

July, 2015

CERTIFICATE

I hereby declare that the thesis entitled "Finite Element Analysis and Mathematical Modeling of a Novel Magnetorheological Honing Process" is an authentic record of my study carried out as requirements for the award of the degree of **Master of Engineering in CAD/CAM and Robotics** at **Thapar University, Patiala** under the supervision of **Dr. Anant Kumar Singh**, Assistant Professor, Mechanical Engineering Department, Thapar University, Patiala during January, 2015 to July, 2015. The matter embodied in this report has not been submitted in partial or full to any other university or institute for the award of any degree.

Date: 14/07/2015

Vishwas Grover

Vishwas Grover

801381025

It is certified that the above statement made by the student is correct to the best of my/our knowledge and belief.

Anant Kumar Singh
14/07/2015

Dr. Anant Kumar Singh
Assistant Professor
Mechanical Engineering Department
Thapar University, Patiala - 147004

Countersigned by

S.K. Mohapatra
Dr. S.K Mohapatra
Professor & Head
Mechanical Engineering Department
Thapar University, Patiala - 147004

S.S. Bhatia
Dr. S.S Bhatia
Dean of Academic Affairs
Thapar University, Patiala -147004

Dedicated to
My Parents

Acknowledgements

I express my sincere gratitude to my guide **Dr. Anant Kumar Singh**, Assistant Professor, Mechanical Engineering Department, Thapar University, Patiala, for their valuable guidance, proper advice and constant encouragement during the course of my thesis work.

I do not find enough words with which I can express my feeling of thanks to the entire faculty and staff of Mechanical Engineering Department, Thapar University, for their help, inspiration and moral support which went a long way in successful completion of thesis work.

(Vishwas Grover)

Abstract

Magnetorheological honing process has been developed for superfinishing of internal surface of cylindrical objects. This process uses magnetorheological polishing fluid to finish the surfaces. Under the influence of magnetic field carbonyl iron particles along with silicon carbide particles present in magnetorheological fluid performs the finishing operation. The performance of finishing action depends on normal force acting on silicon carbide particles which are on workpiece surface. The normal force exerting on silicon carbide particles makes them to intend in workpiece surface and performs finishing on surfaces due to the shear action. Normal force exerting on silicon carbide particles is due to carbonyl iron particles present in magnetorheological fluid under the influence of external magnetic field. In this ME thesis a novel magnetorheological honing tool has been modeled and finite element analysis of magnetorheological honing tool has been done with the help of Maxwell ANSOFT V13 (student version) software. Magnetorheological honing tool dimensions have been optimized on the basis of finite element analysis for magnetic flux density distribution along with workpiece surfaces. Mathematical modeling of magnetically induced forces acting on silicon carbide abrasive particles along with carbonyl iron particles has also been done. Theoretical calculated value of forces on silicon carbide particles along with carbonyl particles has been compared with the value of forces obtained from finite element simulation results in Maxwell ANSOFT V13 software. Value of forces from both (theoretical and finite element analysis) was found in good agreement. Tool dimensions have been finalized for the fabrication as per the optimized value of dimensions obtained from finite element analysis for maximum flux density distribution of in magnetorheological honing tool with workpiece surfaces. The distributions of magnetic flux density gradient were also analyzed in magnetorheological polishing fluid layer between outer tool finishing surface and workpiece surface and it has been found that outer finishing tool surface has maximum flux density gradient and workpiece surface has low flux density gradient. Hence it shows that magnetorheological polishing fluid always retain on the finishing tool surface as it has maximum flux density gradient. This is one of the important requirements to get finishing on any type of workpiece surfaces such as ferromagnetic and non-ferromagnetic materials. Mathematical modeling of magnetically induced normal forces predicts a way to analyze the forces required for finishing action at different process parameters.

Contents

List of Figures	1
List of Tables	5
Nomenclature	6
Acronyms	8
Chapter 1: Introduction	9
1.1 Introduction	9
1.1.1 Traditional Finishing Processes	9
1.1.2 Advance Finishing Processes	11
1.2 Advantages of using Magnetorheological Fluids in Finishing Operations	17
1.3 Application of Magnetorheological Finishing Processes	17
Chapter 2: Literature Review	18
2.1 Literature Review	18
2.2 Research Gap	24
2.3 Objectives of the present work	25
2.4 Methodology of Present Research Work	26
Chapter 3: Finite Element Analysis of Magnetorheological Honing (MRH) Process	27
3.1 Magnetorheological Honing Process	27
3.2 Finite Element Analysis of Magnetorheological Honing Process	28
3.2.1 Selection of material used	28
3.2.2 Electromagnet Model of MRH tool in Maxwell ANSOFT V13 Software	30
3.2.3 Finite Element (FE) Analysis of MRH tool along with Ferromagnetic Workpiece Surface for Magnetic Flux Density	32
3.2.4 Optimizing the Tool Dimensions on the basis of FE Simulation Results	33
3.2.5 Obtained Optimum Dimensions of MRH tool from Maximum Flux Density Distribution Gradient from FE Analysis	48
3.3 FE Analysis for Magnetic Flux Density Distribution in a Cycle of Finishing Operation	49
Chapter 4: Mathematical Modeling of Magnetorheological Honing Process	55
4.1 Mathematical Modeling	55
4.2 Chain Structure and Unit Cell Modeling	56
4.3 Mathematical Modeling of Magnetorheological Honing Tool	57

4.3.1 Number of carbonyl iron particles (CIPs) chains present in the working gap	58
4.3.2 Number of active abrasives per chain of CIPs present on the surface of workpiece	59
4.3.3 Calculation of magnetic flux density	60
4.3.4 Calculation of Force acting on a Carbonyl Iron Particle due to Magnetic Field	66
4.4 Surface roughness modeling	68
4.5 Results and Discussions	70
Chapter 5: Conclusions and Future Scope	73
5.1 Conclusions	73
5.2 Future Scope	74
References	75

List of Figures

Figure 1.1	Lapping Process	10
Figure 1.2	Honing Tool	10
Figure 1.3	Grinding Process	11
Figure 1.4	Experimental setup of 2-way Abrasive Flow Machining Process	12
Figure 1.5	Elastic Emission Machining Process	13
Figure 1.6	MR Polishing Fluid Jet Dispersion	14
Figure 1.7	Schematic Diagram showing MRAFF Process	15
Figure 1.8	Ball End Magnetorheological Finishing Process	16
Figure 1.9	Magnetorheological Abrasive Honing Process	17
Figure 2.1	Surface Roughness Profile (a) Initial (b) After BEMRF at working gap 0.66 mm with F_n - 16.35 N	21
Figure 2.2	Surface roughness values before and after finishing	22
Figure 2.3	Flow Chart for Methodology of Present Research Work	26
Figure 3.1	Inner core of MRH tool	29
Figure 3.2	Inner core of MRH tool along with electromagnet coil	29
Figure 3.3	Schematic diagram of MRH tool retained stiffen MR polishing fluid	30
Figure 3.4	Electromagnet Model of Magnetorheological Honing (MRH) Tool	31
Figure 3.5	Magnetic flux density distribution in MRH tool with ferromagnetic workpiece	32
Figure 3.6	Magnetic Lines of forces direction in FE analysis of MRH tool	33
Figure 3.7	Magnetic flux density distribution of MRH tool (a) with outer core (b) without outer core	34
Figure 3.8	Magnetic flux density distribution of MRH tool for ferromagnetic workpiece surface when MR polishing fluid thickness (a) 1 mm (b) 2 mm (c) 3 mm (d) 4 mm and (e) 5mm	36
Figure 3.9	Magnetic flux density distribution of MRH tool for ferromagnetic workpiece surface when outer core thickness (a) 1 mm (b) 2 mm (c) 3 mm (d) 4 mm and (e) 5mm	37

Figure 3.10	Magnetic flux density distribution of MRH tool for ferromagnetic workpiece surface when spool thickness (a) 1 mm (b) 2 mm (c) 3 mm (d) 4 mm and (e) 5mm	39
Figure 3.11	Magnetic flux density distribution of MRH tool for ferromagnetic workpiece surface when current given to electromagnet coil (a) 1 A (b) 2A (c)3 A (d) 4 A and (e) 5 A	40
Figure 3.12	Magnetic flux density distribution of MRH tool for ferromagnetic workpiece surface when diameter of inner core D_c as (a) 10mm (b) 9mm (c) 8mm (d) 7mm (e) 6mm	42
Figure 3.13	Magnetic flux density distribution of MRH tool for ferromagnetic workpiece surface when diameter of inner core D_c is changing (number of turns of electromagnet coil changes accordingly) as (a) 10mm (b) 9mm (c) 8mm (d) 7mm (e) 6mm	43
Figure 3.14	Magnetic flux density distribution of MRH tool for ferromagnetic workpiece surface when height of inner core H_c (a) 100mm (b) 90mm (c) 80mm (d) 70mm (e) 60mm	45
Figure 3.15	Magnetic flux density distribution of MRH tool for ferromagnetic workpiece surface when number of turns of coil kept constant and varying height of core H_c as (a) 100mm (b) 90mm (c) 80mm (d) 70mm (e) 60mm	47
Figure 3.16	Schematic diagram of MRH tool with ferromagnetic workpiece	48
Figure 3.17	Schematic diagram of Novel Magnetorheological Honing Setup	49
Figure 3.18	MRH tool for ferromagnetic workpiece when base of lower spool is 18mm below from top of the ferromagnetic workpiece (a) Electromagnet model (b) Magnetic flux density distribution	50
Figure 3.19	MRH tool for ferromagnetic workpiece when base of lower spool is 36mm below from top of the ferromagnetic workpiece (a) Electromagnet model (b) Magnetic flux density distribution	50
Figure 3.20	MRH tool for ferromagnetic workpiece when base of lower spool is 54 mm below from top of the ferromagnetic workpiece (a) Electromagnet model (b) Magnetic flux density distribution	51
Figure 3.21	MRH tool for ferromagnetic workpiece when base of MRH tool is	51

	concentric with workpiece (a) Electromagnet model (b) Magnetic flux density distribution	
Figure 3.22	MRH tool for ferromagnetic workpiece when base of lower spool is 18 mm below from bottom of the ferromagnetic workpiece (a) Electromagnet model (b) Magnetic flux density distribution	52
Figure 3.23	MRH tool for ferromagnetic workpiece when base of lower spool is 36 mm below from bottom of the ferromagnetic workpiece (a) Electromagnet model (b) Magnetic flux density distribution	52
Figure 3.24	MRH tool for ferromagnetic workpiece when base of lower spool is 54 mm below from bottom of the ferromagnetic workpiece (a) Electromagnet model (b) Magnetic flux density distribution	53
Figure 3.25	MRH tool for ferromagnetic workpiece when base of lower spool is 62 mm below from bottom of the ferromagnetic workpiece (a) Electromagnet model (b) Magnetic flux density distribution	53
Figure 4.1	Schematic diagram of Magnetorheological Honing tool with ferromagnetic workpiece	55
Figure 4.2	Optical micrograph showing termination of CI particles chain due to the existence of non-magnetic abrasives in MR Fluid	56
Figure 4.3	Carbonyl iron particles and silicon carbide particle arrangement in MRP fluid with repetition of unit cubic cell on application of magnetic field	57
Figure 4.4	The simplified geometric presentation and magnetic circuit of the Magnetorheological Honing Tool with Ferromagnetic Workpiece	61
Figure 4.5	Geometric presentation of Magnetorheological Honing Tool with Ferromagnetic Workpiece	63
Figure 4.6	Distribution of magnetic flux density between MRH tool surface and workpiece surface in MR polishing fluid	65
Figure 4.7	M-B curve for CIP of CS samples	66
Figure 4.8	Distribution of force acting on CI particle between MRH tool surface and ferromagnetic workpiece surface in MR polishing fluid	67
Figure 4.9	(a) Forces on abrasive particles in magnetorheological honing process (b) Calculation of D_i	68
Figure 4.10	(a) Abrasive grain approaching initial peaks/valleys of height/depth and (b) new peak heights updated after one indentation depth (d)	69

Figure 4.11	Electromagnet model of MRH tool having SiC and CIP particles in columnar structure	70
Figure 4.12	Distribution of magnetic flux density MRH tool for ferromagnetic workpiece	71
Figure 4.13	Distribution of magnetic flux density of MRH tool for ferromagnetic workpiece between outer finishing tool surface and ferromagnetic workpiece surface	72

List of Tables

Table 2.1	Surface roughness results	23
Table 3.1	Assigned specifications to the electromagnetic model	28
Table 3.2	Optimum dimensions of MRH Tool obtained from FE simulation of MRH tool with ferromagnetic workpiece	48
Table 4.1	Composition of MR polishing fluid	58

Nomenclature

A	area of the region where MR polishing fluid is present on the outer periphery of the tool (mm^2)
A''	total projected area of abrasive grain, mm^2
A'	projected area of indented part of abrasive in workpiece surface, mm^2
A_k	cross sectional area of the k^{th} link, mm^2
B_{MR}	magnetic flux density in the MR polishing fluid region, T
B_{wrk}	magnetic flux density on workpiece, T
$B_{\text{Outer core}}$	magnetic flux density on outer core of MRH tool, T
D	outer diameter of tool over which MRP-fluid will flow (mm)
D_c	diameter of central part of inner core structure, mm
D_s	diameter of spool, mm
D_i	indentation diameter in, mm
d	depth of indentation of active SiC particle, mm
d_c	diameter of CI particle, μm
d_s	diameter of SiC particle, μm
F_{CIP}	magnetic force on CI particle in magnetic field, Newton
F_{SiC}	magnetic force on SiC particle in magnetic field, Newton
F_i	indentation force acting on workpiece, Newton
F_{normal}	normal force acting on SiC particle, Newton
F_{shear}	shear force acting on SiC particle, Newton
H_k	magnetic field intensity in the k^{th} link of the magnetic circuit
H_{BHN}	workpiece Brinell hardness number, kgf/mm^2
H_c	height of central inner part of core, mm
H_t	total height of the tool, mm
I	current given to the electromagnetic coil, Ampere
l_k	length of k^{th} link of the magnetic circuit, mm
L_s	thickness of the spool, mm
m	mass of CIP, kg
R	radius of complete setup, mm
R_a	surface roughness value

R_c	radius of central part of inner core, mm
R_{normal}	normal force acting on SiC particle by workpiece surface, Newton
R_{shear}	shear force acting on SiC particle by workpiece surface, N
t_o	thickness of outer core, mm
t_{wrk}	thickness of workpiece, mm
N	number of turns of coil
N_{AAB}	number of active abrasives present on the workpiece surface
N_{CIP}	number of carbonyl iron particles (CIPs) in volume V of MRP-fluid
$N_{(\text{CIP})\text{chains}}$	total number of CIPs chains formed in given volume V of MRP- fluid
N_g	number of active abrasive particles/stroke of finishing process
N_{SiC}	number of silicon carbide particle (SiC) in volume V of MRP-fluid
N'	number of data points taken into account for finishing action
V	total volume of MR polishing fluid in working gap, mm^3
y	thickness of MRP- fluid in between tool and workpiece, mm
w_c	width of coil, mm
Y_i	roughness profile height at the data points

Greek letters

χ_m	magnetic susceptibility of carbonyl iron particles (CIPs), m^3/kg
Φ	magnetic flux of the circuit
μ_k	relative permeability of the k^{th} link, H/m
μ_0	magnetic permeability of free space, H/m
σ_y	yield stress of workpiece in shear
τ_y	magnetorheological polishing fluid shear stress

Acronyms

BEMRF	Ball end magnetorheological finishing
CIP	Carbonyl iron particles
CLA	Centre line average
FE	Finite element
MR	Magnetorheological
MRH	Magnetorheological honing
MRAFF	Magnetorheological abrasive flow finishing
MRAH	Magnetorheological abrasive honing
MRR	Material removal rate
SiC	Silicon carbide
SWG	Standard wire gauge

Chapter-1

Introduction

1.1 Introduction

Finishing of components which needs higher accuracy is a very difficult and more time taking task in manufacturing industry. Generally, pre-machined specimens are processes with finishing processes like grinding, honing, superfinishing, grinding, lapping which use strong tools. There are some limitations with these traditional processes that these processes cannot finish complex surfaces, cannot finish components to precisely nanolevel and can sometimes result in damaged surfaces. To resolve these problems, several attempts have been performed to improve these finishing processes but could not meet increasing demand of finishing of complex geometries precisely. These finishing processes may even lead to damaged surfaces. Even if these processes perform precise finishing, these require expensive equipment and labour.

1.1.1 Traditional Finishing Processes

Several finishing processes are available to finish the surface of workpiece like honing, grinding, lapping etc. These are basic finishing processes which are generally used for pre-machined surfaces. These processes have limitation that forces applied for finishing operation is not controllable that is why it may lead to failure of workpiece. Moreover, finishing obtained from these processes is not so good. Various commonly used traditional finishing processes are given below.

(a)Lapping

Lapping is a finishing process which is used to produce flat or smooth surface. Finishing action is done by loose abrasive particles. Abrasives are suppressed on workpiece surface by a tool called lap (or press plate) and are rotated on workpiece surface as shown in Fig 1.1. Lapping can remove material up to ranges from 0.03mm to 0.3mm. Most commonly used material for lapping tool is cast iron. But soft steel and copper can also be used as a lapping tool.

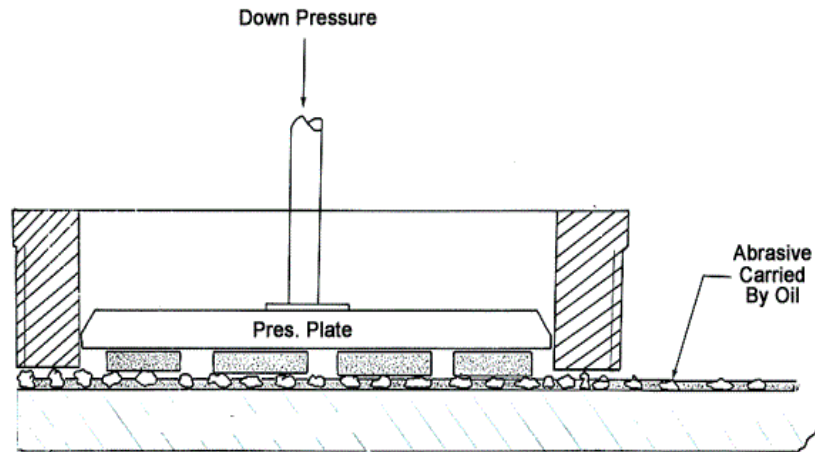


Figure 1.1: Lapping Process [http://www.columbiagrinding.com/images/lapping_diagram.gif]

(b) Honing

Honing is a process which is used for finishing of internal surface of cylindrical workpiece. Finishing is performed by abrasive stone attached on tool called honing tool which is allowed to rotate and reciprocate inside cylindrical workpiece as shown in Fig. 1.2. Honing process is used for metallic as well as non-metallic workpiece surface. The pressure exerted by honing tool on surface of workpiece is more than lapping. Honing process covers a large area of workpiece therefore the generation of temp. is low. Limitation of the honing process is the low finishing rate and also only used for the cylindrical surfaces only.

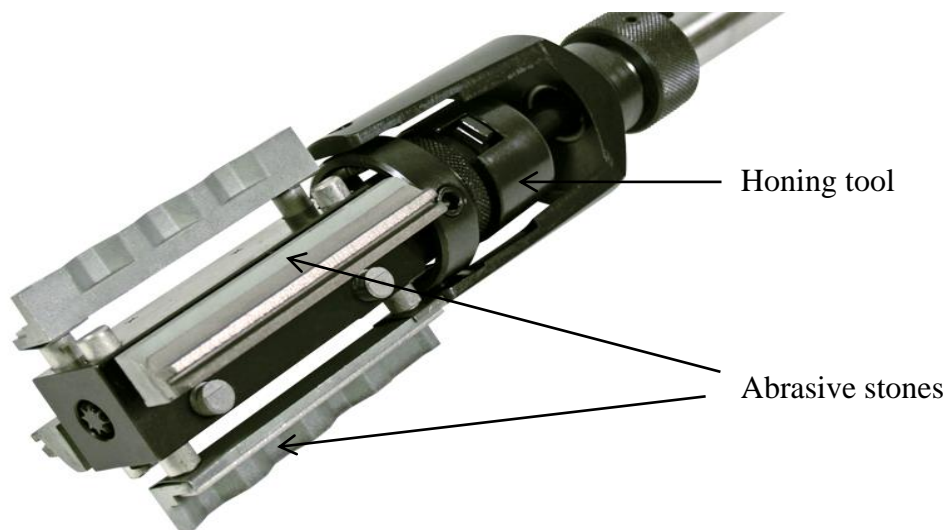


Figure 1.2: Honing Tool

[[https://en.wikipedia.org/wiki/Honing_\(metalworking\)#/media/File:WVN_Diam.png](https://en.wikipedia.org/wiki/Honing_(metalworking)#/media/File:WVN_Diam.png)]

Limitation of the honing process is the low finishing rate and also only used for the cylindrical surfaces only.

(c) Grinding

Grinding is a finishing process in which material removal is done by relative movement of grinding wheel (having abrasive particles) on surface to be finish as shown in Fig. 1.3. Grinding process can finish the surface value up to roughness value of $1\ \mu\text{m}$. Grinding wheel get blunt after some time and needs to be regrind at regular intervals. It is done by diamond tool. It removes the fractured abrasives from the bond.

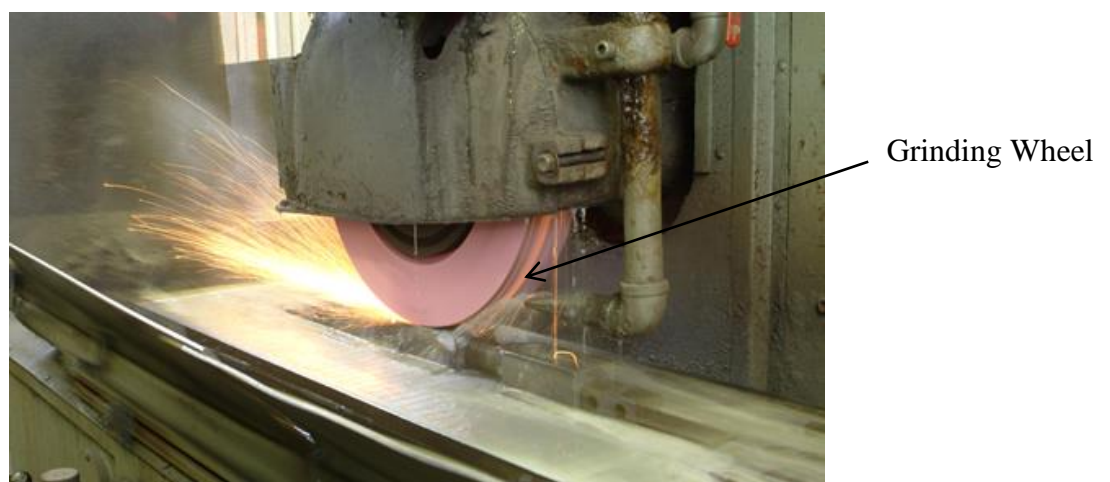


Figure 1.3: Grinding process [<http://www.watsongrinding.com/wp-content/uploads/2011/12/Grinding.jpg>]

Process of regrinding of grinding wheel is quite expensive and time consuming. Normal force acting in grinding operation is high that leads to the sub surface damage.

1.1.2 Advance Finishing Processes

Processes which are used to finish the surface precisely to nanometer surface roughness are called advance finishing processes. In these processes finishing action is done by small abrasive particles. Force acting on workpiece surface is quite small as it is applied by abrasive particles so there is less chance of surface rupture or fracture. It also leads to increase of tool life.

Advanced finishing processes are divided in two categories:

- 1) Without external control of forces.
- 2) With external control of forces.

1) Advance Finishing Processes Without External Control of Forces

These are the finishing processes which are used for ultrafine finishing of surfaces but finishing force exerted on surface of workpiece due to the abrasives particles cannot be controlled. Force exerting on surface of workpiece is not uniform. Some of the examples of advance finishing processes without external control of forces are given below:

➤ Abrasive Flow Machining Process (AFM)

Abrasive flow machining process is the finishing process which is used to deburr and polish internal surfaces of cylindrical objects. AFM process is of three type 1-way AFM, 2-way AFM and orbital AFM. A 2-way AFM process is shown in Fig. 1.4 in which finishing is performed by abrasive particles (in a viscoelastic polymeric medium) which are allowed to reciprocate up and down with the help of two vertically opposed pistons. Good abrasion is obtained inside the cylinder where fluidic medium is allowed to flow through narrow passage. AFM process can finish the surface as good as $0.05 \mu\text{m}$.

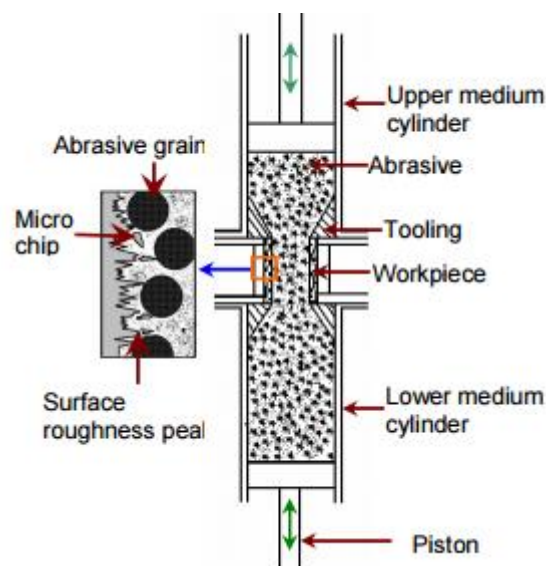


Figure 1.4: Experimental setup of 2-way Abrasive Flow Machining process [Jain et al., 1999]

➤ Elastic Emission Machining

This method has the capability to remove the material from the workpiece surface at the atomic level by mechanical action and produce the physically undisturbed surface. In this process ultrafine abrasive particle strikes the individual atom and separate out from the parent surface as shown in Figure 1.5. It has been found that the process of material elimination material removal ps is a surface energy phenomenon in which every abrasive particle

eliminates a number of atoms after make contact with surface of the workpiece surface [Mori et. al, 1987].

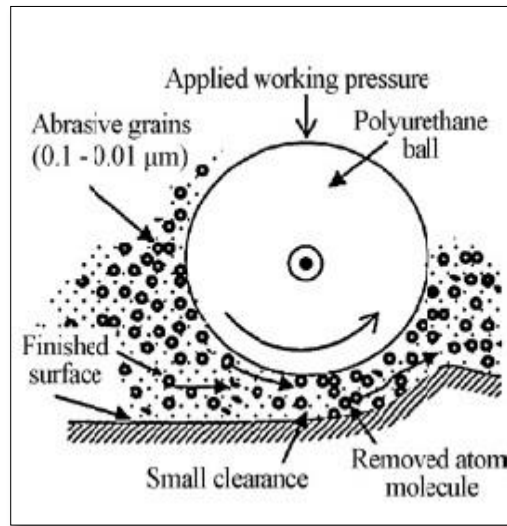


Figure 1.5: Elastic Emission Machining Process [Jain, 2009]

2) Advance Finishing Processes with External Control of Forces

Several advance finishing operations have been developed in which force exerted on surface of workpiece can be controlled by controlling current given to electromagnet coil or by changing the working gap between the workpiece and tool. Such finishing processes make use of a special kind of smart fluid called magnetorheological (MR) fluid. MR polishing fluid is special kind of fluid which is made up of (CIPs) and (SiCs) particles with base fluid (grease, paraffin oil). In the presence of magnetic field (created by permanent magnet or electromagnet coil), carbonyl iron particles (CIPs) get aligned in a straight line due to dipolar moment. Due to magnetic field MR polishing fluid stiffens. Silicon carbide particles (SiCs) get entrapped in between chain of CIPs.

In finishing processes with external control of forces, forces acting on workpiece for finishing action can be controlled by varying the current given to the electromagnet coil. With the change in the electric current, the magnetic flux density in the finishing area due to which normal force acted by the abrasives on the workpiece changes [Jain, 2009]. Also, as the current increases, magnetic flux due to electromagnet coil increases. Due to more magnetic flux, MR polishing fluid gets stiffer and gives good finishing action. Several advance finishing processes with external control of forces are given below.

- A. Magnetorheological Jet Finishing Process.
- B. Magnetorheological Abrasive Flow Finishing (MRAFF) Process.

C. Ball end MR Finishing (BEMRF) Process

D. Magnetorheological Abrasive Honing (MRAH) Process

A. Magnetorheological Jet Finishing Process

Jet finishing process is a process in which finishing is done by pressurized fluid jet on the surface to be finish. Fluid has a property that it starts losing its coherence as it comes out from the nozzle due to surface tension and pressure gradients. The fluid disturbance gets highly increase when velocity of jet increases. Due to this disturbance high speed jet of liquid get breaks up into droplets and gets spread out. These spread out droplets of fluid performs the finishing action. Diameter of jet coming out from nozzle of very small diameter and flow of fluid is highly pressurized to get precise finishing. Such jets of fluid also have abrasive particles (having high kinetic energy) with them which chips off the material from surface.

As the distance between nozzle and the workpiece surface increases, coming out fluid jet get highly unstable which is not acceptable for getting high precision finishing with high precision. For getting a coherent jet fluid jet velocity cannot be reduced but it is also not acceptable because it results in low impact force and therefore low MRR. In order to improve dispersion of liquid fluid coming out from nozzle, a novel method of magnetorheological jet finishing process was developed in which CI particles are mixed with fluid and fluid is called MR polishing fluid. MR polishing fluid is used in presence of magnetic field. Due to presence of magnetic field MR polishing fluid does not get dispersed off and give better finishing action. A schematic diagram showing improvement in dispersion of liquid fluid is shown in Fig. 1.6.

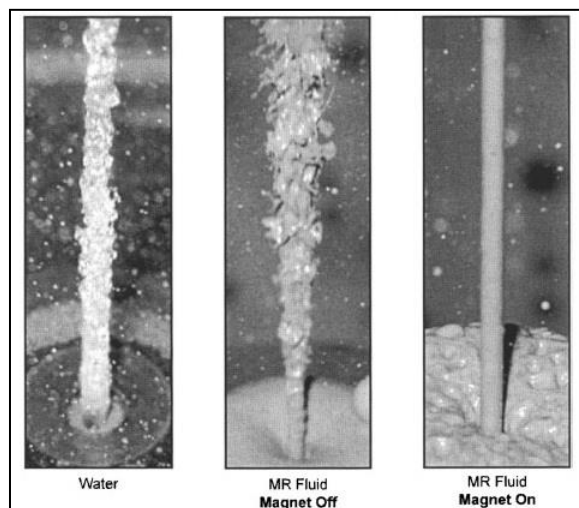


Figure 1.6: MR Polishing Fluid Jet Dispersion [Kordonski et al., 2004]

B. Magnetorheological Abrasive Flow Finishing (MRAFF) process

Magnetorheological abrasive flow finishing process is a process which is used for finishing for internal surface of cylindrical workpiece. Under the action of magnetic field, finishing is performed by MR polishing fluid. It is advancement to honing process in which finishing force can be regulated by varying the magnetic field. MR polishing fluid is allowed to rotate inside the cylindrical workpiece. Magnetic field is generated by externally placed electromagnet. Under the action of magnetic field MR polishing fluid gets stiff enough to perform the finishing action. A schematic diagram showing MRAFF process is shown in Fig 1.7.

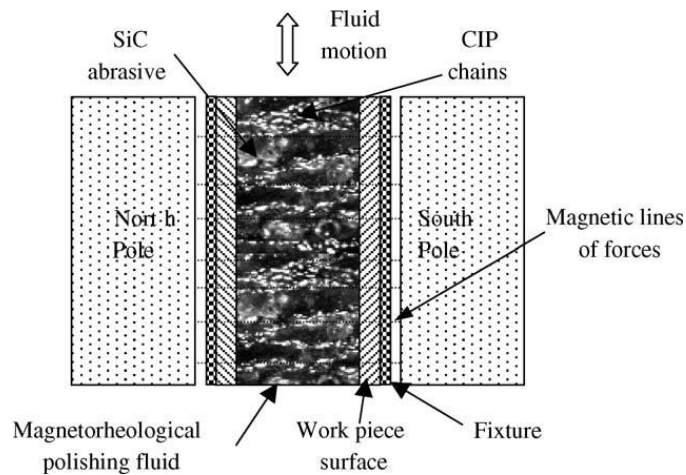


Figure 1.7: Schematic Diagram showing MRAFF Process [Jha and Jain, 2006]

C. Ball End Magnetorheological Finishing (BEMRF) Process

It is the finishing process which is used to precisely finish 3-D surface with the help of MR polishing fluid. A core is rotated over the workpiece surface and MR polishing fluid is allowed to flow through core. Magnetic field is produced by electromagnet coil wound over the core. In the presence of magnetic field, MR polishing fluid gets stiff enough and forms a ball shaped structure which performs the finishing action. Due to this ball shaped structure this process is called ball end magnetorheological finishing process (BEMRF). Normal force acting on workpiece surface by MR polishing fluid can be controlled by changing electromagnet current given to the coil. The setup of ball end magnetorheological finishing process is given in Fig. 1.8.

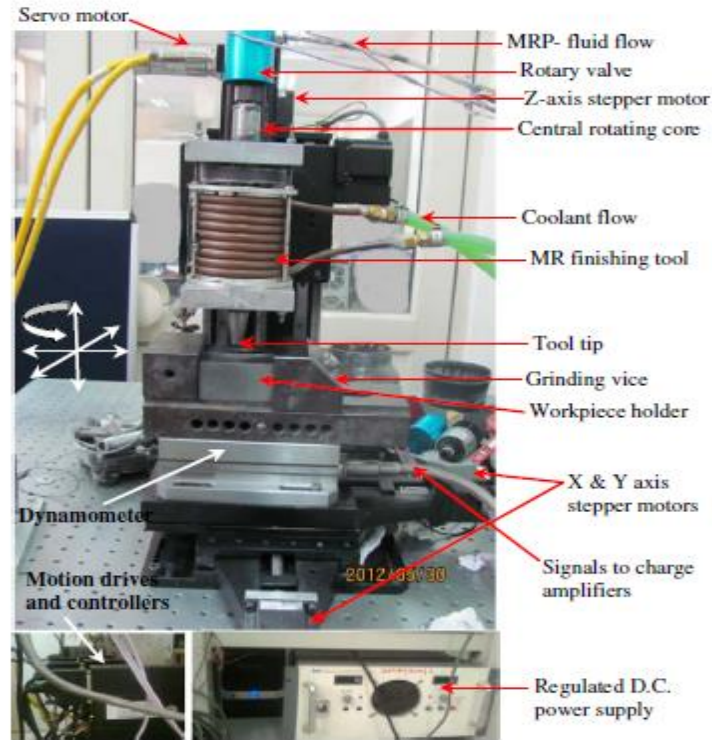


Figure 1.8: Ball End Magnetorheological Finishing process [Singh et al., 2012]

D. Magneto Rheological Abrasive Honing (MRAH) Process

Magnetorheological abrasive honing process is a finishing process which is used to finish external surface of cylindrical objects. Cylindrical workpiece is attached with spindle and allowed to rotate in MR polishing fluid as shown in Fig. 1.9. MR polishing fluid flows over the workpiece surface and is pushed up and down with the help of plunger. Magnetic field is produced by external permanent magnet which is placed across outer cylinder. Under the influence of magnetic field, CI particles present in MR polishing fluid undergoes dipolar interaction and form a chain like structure. Due to rotatory and reciprocatory motion of MR polishing fluid abrasive present in MR polishing fluid apply normal and tangential force on surface of workpiece which results in removal of workpiece and performs finishing action.

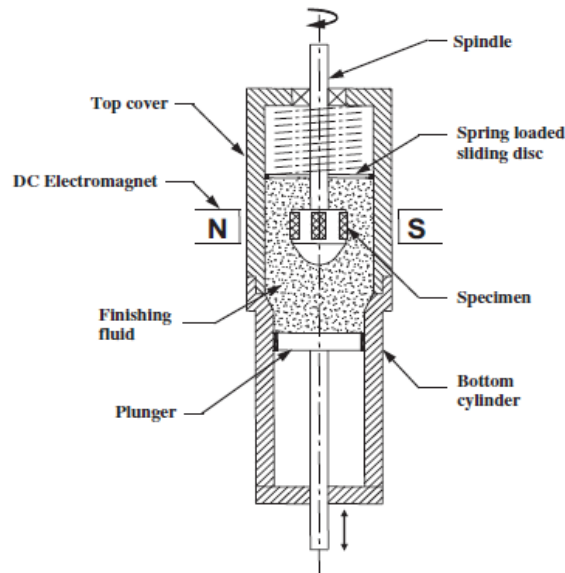


Figure 1.9: Magnetorheological Abrasive Honing Process [Sadiq and Shunmugam, 2010]

1.2 Advantages of using Magnetorheological Fluids in Finishing Operations

Using MR polishing fluids in finishing operations have the following advantages over conventional finishing processes.

- Finishing forces exerted on the surface of workpiece can be regulated by controlling the magnetizing current as per the properties of workpiece surfaces. These are not possible in conventional finishing processes.
- MR finishing is capable of producing surface roughness upto nano level
- MR finishing processes are used to precisely finish the surfaces of any shape.

1.3 Applications of Magnetorheological Finishing Processes

- Optical industries
- Aerospace and automobile industries
- Medical industries
- Defense etc.

Chapter-2

Literature Review

2.1 Literature Review

Researchers have developed many conventional and advance ultrafine finishing processes as per the requirement of surface finishing at various level and applications. These have been developed from traditional to ultrafine finishing processes. Traditional finishing processes are developed such as grinding [Wu et al., 2007], honing [Nowicki, 1993], ball burnishing [Shiou, 2003], flexible abrasive tools [Cho et al., 2002], etc. However, the requirement of ultrafine finishing of surface was still an issue due to various reasons like high temp, intended abrasive particles and uncontrollable finishing forces etc. For these problems several advance finishing processes were developed. In this chapter, the literature review of various authors in the field of advanced finishing processes (with/without the help of magnetic properties) have been discussed and their brief observations have been drawn from the authors work and are represented here for better understanding.

[Gheisari et al., 2014] developed a magnetorheological finishing process for ultra-precision finishing of Aluminum work material (cylindrical type). The MR fluid consists of water based suspension of micron sized diamond particles. The process parameters were (current- 9A and working gap- 5 mm). The initial surface roughness of the work material was 170 nm. The experimentation was conducted in three sets. In first set, the work material speed varies from 250-1000 rpm. In second set, the process time varies from 20-100 min. In third case, the effect of a fast RAM on the surface roughness was considered. The results concluded that with the increase in rotational speed (1000 rpm), the surface roughness value improves by 40 nm. With the increase in finishing time (90 min), the surface roughness value decreases to 42 nm whereas, when the fast RAM (with 0.5 m/sec) was applied, the surface roughness value improves by 78 nm.

[Cheng et al., 2008] worked on wheel shaped polishing tool for finishing of K9 glass mirror by the use of MR polishing fluid (usually a mixture of 33.84% carbonyl iron powder, 57.34% silicon oil, 2.82% stabilizing agent and 6% cerium agent). The experimental studies were conducted in two sets (with/without abrasives). The results concluded that the surface

roughness decreases to 0.47 nm (with viscosity- 8.9 Pa, voltage- 2V, time- 20 min).

[Seok et al., 2007] presented a study on the fabrication of curved surfaces by using a magnetorheological fluid finishing process. In this research paper the fabrication method of curved surfaces depends on the silicon-based micro structures by magnetorheological finishing process was studied. The explanations were made between the procedures of analysis and evaluation of surface characteristics of the workpiece. The effect of the magnetic field around the tool assembly was investigated using a finite element method.

[Judal et al., 2013] developed a new vibration assisted magnetic abrasive finishing process for finishing of aluminium workpiece. The finishing was carried out with the help of steel grit and Al_2O_3 abrasive. The effect of different process parameters such as rotational speed, frequency, magnetic flux density and size of abrasive particles on material removal rate was investigated. The result concluded that with the increase in rotation speed and magnetic flux density and frequency of vibration, the value of material removal rate increases. The surface roughness value Ra decreases to 0.18 μm .

[Wang and Hu, 2005] compare the performance of surface roughness and MRR with finishing time by using a magnetic assisted finishing process for finishing of Ly12 aluminum alloy, 316L stainless steel and H62 brass. The experimentation was carried out with 4 different types of abrasive particle were $\text{Al}_2\text{O}_3/\text{Fe}$ (20% Al_2O_3), TiC/Fe (20% TiC), TiC/Fe (35% TiC), TiC/Fe (7% TiC) along with a finishing fluid (stearinic acid and transformer oil). The results concluded that the value of MRR increases whereas the surface roughness value decreases with increase in finishing time.

[Jang et al., 2012] performed deburring of microparts using a magnetorheological fluid. In this research paper a new deburring process was found by utilizing a magnetorheological fluid and then it was applied it to the production of micromolds. This magnetorheological fluid was one type of functional fluid with a variable yield stress and it was controlled by an external magnetic field. Two material removal mechanisms were proposed in this paper where extensive yielding of material was effective for the deburring sheet shaped burrs and abrasive wear were effective for deburring protrusion-shaped burrs.

[**Sidpara and Jain, 2012**] evaluated the theoretical and experimental analysis of normal and tangential forces by using magnetorheological finishing process for finishing of single crystal silicon. The finishing was done by MR polishing fluid (usually a mixture of CIPs, abrasive particles and glycerol).

[**Wang and Lee, 2009**] worked on magnetic finishing process for precise finishing of cylindrical type (SKD-110 mild steel. The finishing medium includes silicone gel, steel grid (SG) and silicon carbide. The results concluded that the surface roughness with magnetic field shows better results. With the increase in the quantity of SiC particles, the surface roughness decreases, whereas MRR increases.

[**Sidpara and Jain, 2013**] performed an experiment to measure the forces on the freeform surface in real time. The angles of curvature of the workpiece, rotational speed of the tool and feed rate on normal, tangential and axial forces which are the parameters of the process were given by the researchers. It was found that the normal force was more dominant as compared to other forces. Model of normal force and tangential force acting on the workpiece was also proposed to improve the understanding of the workpiece abrasive particles interaction in the MR polishing fluid which was based on finishing process. Theoretical and experimental results were carried out and compared to validate the proposed models

[**Sadiq and Shunmugam, 2010**] in this research paper observed that the change in the surface finish on magnetic specimens was insignificant, whereas the surface finish on non-magnetic specimens improves appreciably. A improved method of introducing magnetic specimens along with non-magnetic specimens was used in this paper and the magnetic field near the non-magnetic specimens was enhanced appreciably. The results obtained on the non-magnetic specimens were found better.

[**Jain, 2009**] showed an overview of various flowing abrasive based MNM processes. This paper also proposed a generalized mechanism of material removal technique for this process. By using a nanometer size abrasive particles EEM resulted in surface finish of the order of sub-nanometer level. Except two processes (AFF and EEM), all other processes mentioned above had been used a medium whose properties can be controlled externally with the help of magnetic field. The forces acting on an abrasive particle and the amount of material removed

was also controlled by the proposed method.

[Cheng et al. 2010] developed a dual axis MRF tool with internal magnet for finishing of BK7 mirror. The finishing was carried out with the help of MR polishing fluid (includes 10% CeO₂ abrasive particles). The mathematical modeling was carried out in order to calculate material removal. The process parameters were (magnetic field strength- 860KA/m and polishing time- 1 min). The results concluded that the surface roughness value decreases from 328.42 nm to 42.93 nm.

[Singh et al., 2013] compared the theoretical and experimental experiments on MRR with different working gaps by using ball-end MR finishing tool for finishing ferromagnetic material. The theoretical observation was carried out by using the mathematical formulas for calculating the normal forces at different working gap. The finishing was carried out with MR polishing fluid (usually a mixture of 20% CIPs, 20% SiC abrasive powder and 60% visco plastic base medium). The results concluded that the surface roughness decrease to 0.028 μm with 0.66 mm working gap as illustrated in Fig. 2.1 below.

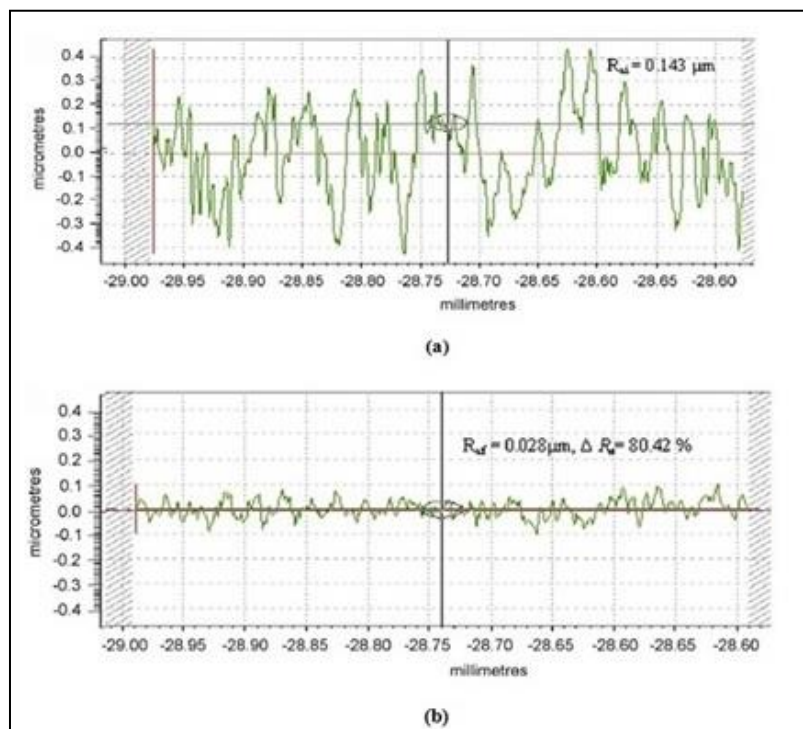


Figure 2.1: Surface Roughness Profile (a) Initial (b) After BEMRF at working gap 0.66 mm with Fn- 16.35 N [Singh et al., 2013]

[Singh et al., 2004] worked on magnetic abrasive process in order to determine the effect of process variable on the surface finish by using a mixture of 75% iron and 25% SiC with different parameters. It is concluded that the value of surface roughness ΔRa was better within the parameters of voltage-11.5 V, working gap-1.25 mm, speed-180 RPM improving the surface roughness values as shown in Fig. 2.2 below.

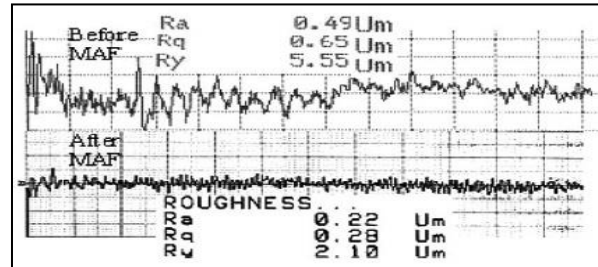


Figure 2.2: Surface roughness values before and after finishing [Singh *et al.*, 2004]

[Pattanayak and Aggarwal, 2005] showed development of Magnetorheological Finishing (MRF) process for freeform surfaces. In the present work, a setup had been developed for MRF application using a pillar drilling machine. Experiments were conducted to finish free form jobs of copper material using the developed setup. The effects of various process parameters such as composition of the MR polishing fluid, rotational speed of work and vessel containing MR polishing fluid and mesh size of abrasives on surface finish were explored.

[Schmitt et al., 2013] performed their experiment on a commercially available honing machine for finishing of 16MnCr5 hardened steel. The honing machine uses a single stone tool equipped with a honing stone containing CBN with abrasive in a metallic sintered bond and a two guide stone with a diamond grains. The experimental parameters were speed- 1600 rpm, stroke velocity- 0.26 m/sec and material removal- 3 mm respectively. The experimentation was carried by the use of 3 closed loop controller (P1, P2 and P3) for controlling the process. The result concluded that the straightness was slightly better for P3 controller, whereas parallelity was better for P2 controller. The (P2 and P3) controller provides the better results as compared to P1 controller.

[Jha and Jain, 2006] evaluated the effect of different grades of CIPs particles (CS and HS) on the surface finish by using magnetorheological abrasive flow finishing process for finishing of stainless steel material. MR polishing fluid (usually a mixture of 20% CIPs, 20% SiC abrasive powder and 60% visco plastic base medium) with which the finishing was done.

The results concluded that higher improvement in surface roughness between 0.32-0.09 μm was made by using CIPs (CS) with SiC-800 mesh size as illustrated in Table 2.1.

Table 2.1: Surface roughness results [Jha and Jain, 2006]

Expt. No.	CIP dia. (D_{CIP}) (μm)	SiC dia. (D_{SiC}) (μm)	$D_{\text{CIP}}/D_{\text{SiC}}$	Initial Ra (μm)	Final Ra (μm)	ΔRa^a (μm)	$\%\Delta\text{Ra}$
1.	18.0 (CS)	19.00	0.95	0.32	0.09	-0.23	-17.87
2.	18.0 (CS)	12.67	1.42	0.28	0.17	-0.11	-39.28
3.	18.0 (CS)	7.50	2.40	0.31	0.23	-0.08	-25.80
4.	3.5 (HS)	19.00	0.18	0.26	0.23	-0.03	-11.54
5.	3.5 (HS)	12.67	0.28	0.28	0.24	-0.04	-14.28
6.	3.5 (HS)	7.50	0.47	0.25	0.24	-0.01	-4.00

[Das et al., 2010] worked on rotational magnetorheological abrasive flow finishing process for finishing of stainless steel work material. The finishing was carried out with the help of MR polishing (usually contains 26.6% Fe powder, 13.5% SiC abrasive with base fluid). The preliminary experimentation along with design of experiment and response surface regression analysis were also carried out in order to determine the effect of abrasive particle size, rotational per minute of magnet and finishing time on the surface roughness. The results concluded that with the increase in RPM (up to 150) and finishing time (1600 sec) the surface roughness founds to be better, whereas with the decrease in abrasive particle size (150), the surface roughness founds to be better

[Kang et al., 2012] designed and developed a newly built magnetic abrasive finishing (with double dipole tip set) for finishing of austenite 304 stainless steel tubes. The mixed type magnetic abrasive consists of (80% iron particles and 20% magnetic abrasive) along with a soluble type barrel finishing compound. The process parameters were (magnetic flux- 1.26-1.29 T, speed- 500-30000 rpm, processing time- 10 to 20 min and workpiece pole tip clearance- 0.3 mm). The initial surface roughness of 304 stainless steel was 2-3 μm . The results concluded that at 10000 rpm the surface roughness decrease to 0.1 μm (for 10 min) whereas, the surface roughness at 10000 rpm decrease to 0.11 μm (20 min).

2.2 Research Gap

From the literature review it has been seen that many magnetorheological finishing processes are available for the finishing of surfaces of cylinder such as magnetorheological abrasive flow finishing [Jha and Jain, 2006] magnetorheological abrasive honing process [Sadiq and Shunmugam, 2010] etc. But in these processes, magnet poles were kept externally the outer surface of workpiece which results in higher magnetic flux density gradient on the ferromagnetic workpiece surfaces and less magnetic flux density gradient in MR polishing fluid. Therefore MR polishing fluid get attached on the ferromagnetic workpiece and MR polishing fluid could not able to finish the surfaces as there was found no relative motion between the workpiece surfaces and MR polishing fluid. Hence, these processes are not good for finishing of ferromagnetic workpiece surfaces because under the influence of magnetic field, MR polishing fluid gets stick up to the workpiece surface as magnitude of magnetic flux density is more on surface of workpiece. As magnitude of magnetic flux density is low in MR polishing fluid region so MR polishing fluid does get stiff enough to perform good finishing action.

To overcome these limitations a novel process has been developed using MR polishing fluid for finishing of internal surfaces of cylindrical objects named as magnetorheological honing (MRH) process. The main advantages of MRH process are as follows:

- In this process electromagnet was not kept externally outside the workpiece surfaces. A novel magnetorheological honing tool has been developed where electromagnet coil was kept inside the finishing tool itself. Therefore, maximum flux density gradient can be found always on the finishing tool as compared to ferromagnetic and non-ferromagnetic workpiece surfaces.
- Magnitude of magnetic flux density is more in MR polishing fluid region because magnetic field is produced by electromagnet coil. So MR polishing fluid stiffs enough to perform the finishing action.
- Strength of magnetic field can be increased by increasing current given to the electromagnet coil as per the requirement.
- As magnitude of magnetic flux density is more in MR polishing fluid as compared to the workpiece so there is no problem of sticking of CI particles on workpiece surface.
- This process can be used for ferromagnetic and non-ferromagnetic workpiece.

2.3 Objectives of the present work

The main objectives for development of magnetorheological honing process are given below:

- To design and optimize the dimensions of magnetorheological honing tool using MAXWELL ANSOFT V13 software.
- To calculate the magnetically induced normal forces during finishing operation on active abrasive particles developing a mathematical model.
- To verify calculated theoretical value of forces on abrasives with forces obtained from finite element (FE) analysis in MAXWELL ANSOFT V13software.
- To verify the maximum flux density gradient on the magnetorheological honing tool surface as compared to ferromagnetic workpiece surface.

2.4 Methodology of Present Research Work

Methodology followed for performing present research work is in the following way

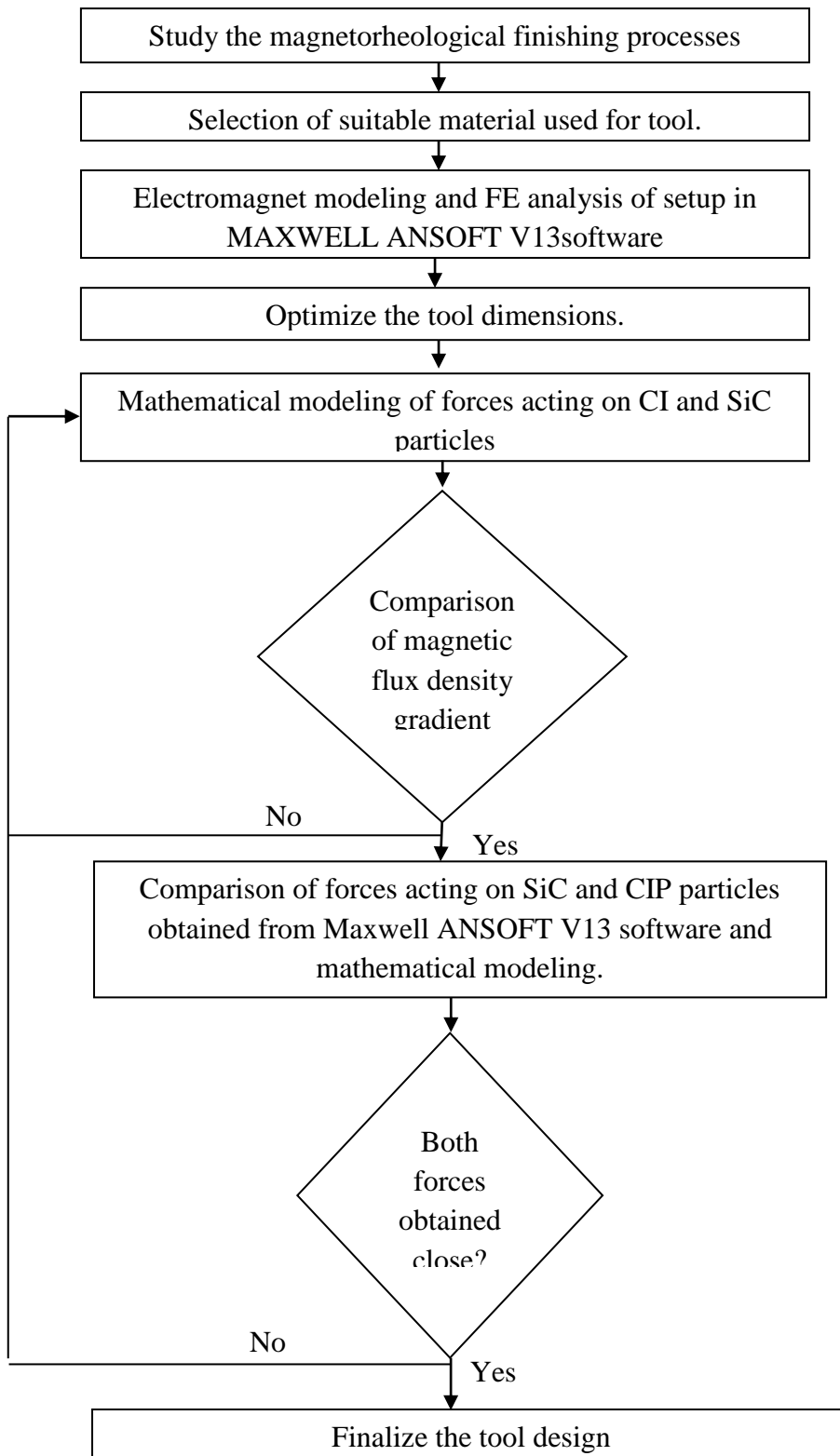


Figure 2.3: Flow Chart for Methodology of Present Research Work

Chapter-3

Finite Element Analysis of Magnetorheological Honing (MRH) Process

3.1 Magnetorheological Honing Process

Magnetorheological honing (MRH) process is the advanced finishing operation which is utilized to finish the internal cylindrical surfaces objects to a precisely nano level. It is the process in which finishing is done with MR polishing fluid under the influence of magnetic field. Magnetorheological honing (MRH) tool is allowed to rotate and reciprocate inside the cylindrical workpiece. Under the influence of magnetic field, MR polishing fluid gets stiff and performs the finishing action. CIP chain structure tightly grips the abrasive particles (which are on the cylindrical workpiece surface) [Singh et. al, 2012]. These gripped abrasive particles due to the rotation and reciprocation of MRH tool performs the finishing action. At present there is a great need of super finishing of cylindrical objects. There are many practical applications of super finishing required for cylindrical objects as listed below:

- Hydraulic cylinders
- Defense rifle barrel
- Cylindrical blocks of engines
- Air bearing
- Exhaust manifold of engines

In this chapter design optimization of magnetorheological honing tool has been done on the basis of getting maximum magnetic flux density on the outer surface of the tool. A software Maxwell ANSOFT V13 is used for analysis of magnetic flux density. Specification assigned to generate the electromagnet model of magnetorheological honing (MRH) tool is shown in Table 3.1

Table 3.1: Assigned specifications to the electromagnetic model

Specification	Material	Relative Permeability	Current
Electromagnet coil	Copper	1	4 A
Inner core	Iron	600	
Outer core	Iron	600	
MR polishing fluid	MR polishing fluid	5	
Workpiece	Iron	600	

3.2 Finite Element Analysis of Magnetorheological Honing Process

Steps involved in design finite element analysis of magnetorheological honing process are as follows:-

- Selection of material suitable for making tool.
- Create the electromagnet model of MRH tool in MAXWELL ANSOFT V13 (student version) software.
- Magneto static simulation of the tool for distribution of magnetic flux density.
- Optimizing MRH tool dimensions on the basis of FE simulation results.
- Finalizing and validate tool dimensions.

In MAXWELL ANSOFT V13 (student version) software tool is modeled and simulated, and on the basis of magnetic flux density simulations results changes in tool design has been done. Main objective to obtain from simulation results is get maximum magnetic field. Changes are made in the dimensions where getting more magnetic field. The more magnetic field is obtained, the more beneficial it will be in finishing operation as with in presence of high magnetic field, MR polishing fluid gets more stiff and performs the better finishing action.

3.2.1 Selection of material used

For performing simulation in MAXWELL ANSOFT V13 material is need to be assigned to the different parts. Material selected for tool and workpiece is iron with relative permeability

of 600. The relative permeability of materials in MRH tool with ferromagnetic workpiece has been assigned from library provided by Maxwell ANSOFT V13.

Different parts of Magnetorheological Honing (MRH) tool are shown below:

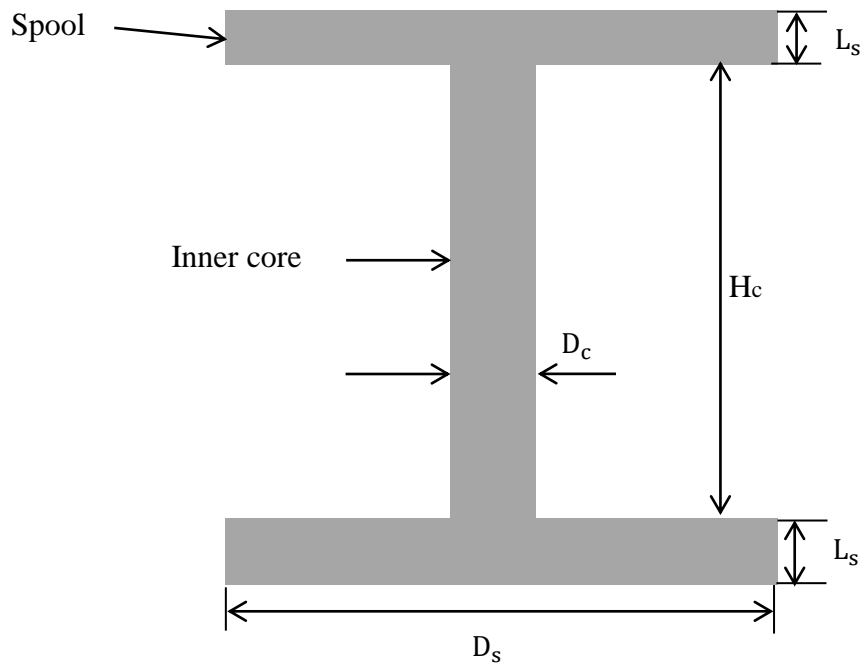


Figure 3.1: Inner core of MRH tool

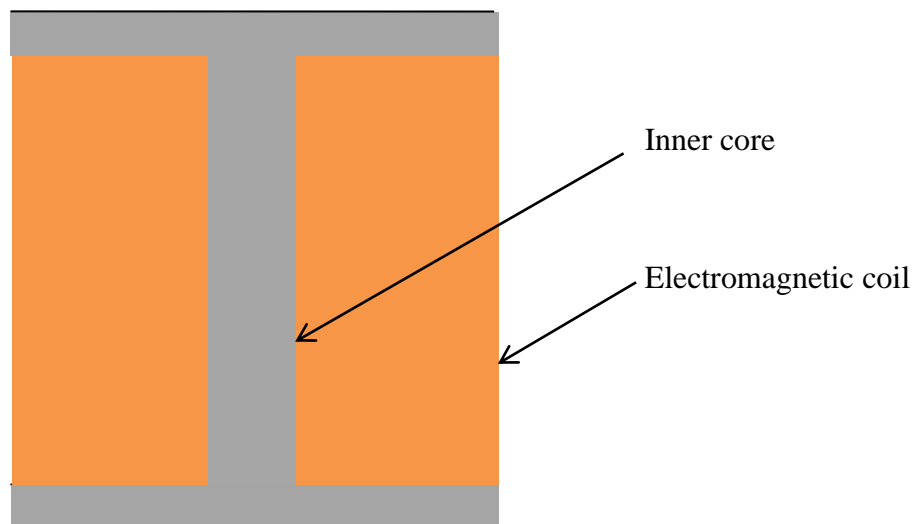


Figure 3.2: Inner core of MRH tool along with electromagnetic coil

Value of relative permeability of materials has been referred [Singh et al., 2012]. Electromagnetic coil which is wound over the core is made up of copper with relative permeability 1. MR polishing fluid flowing outside the tool has the relative permeability of 5.

These parameters are assigned to the materials for firstly performing the simulation. Later on the basis of FE analysis results, changes have been done in these parameters accordingly to get the required results i.e. where field intensity is more or getting more force on workpiece.

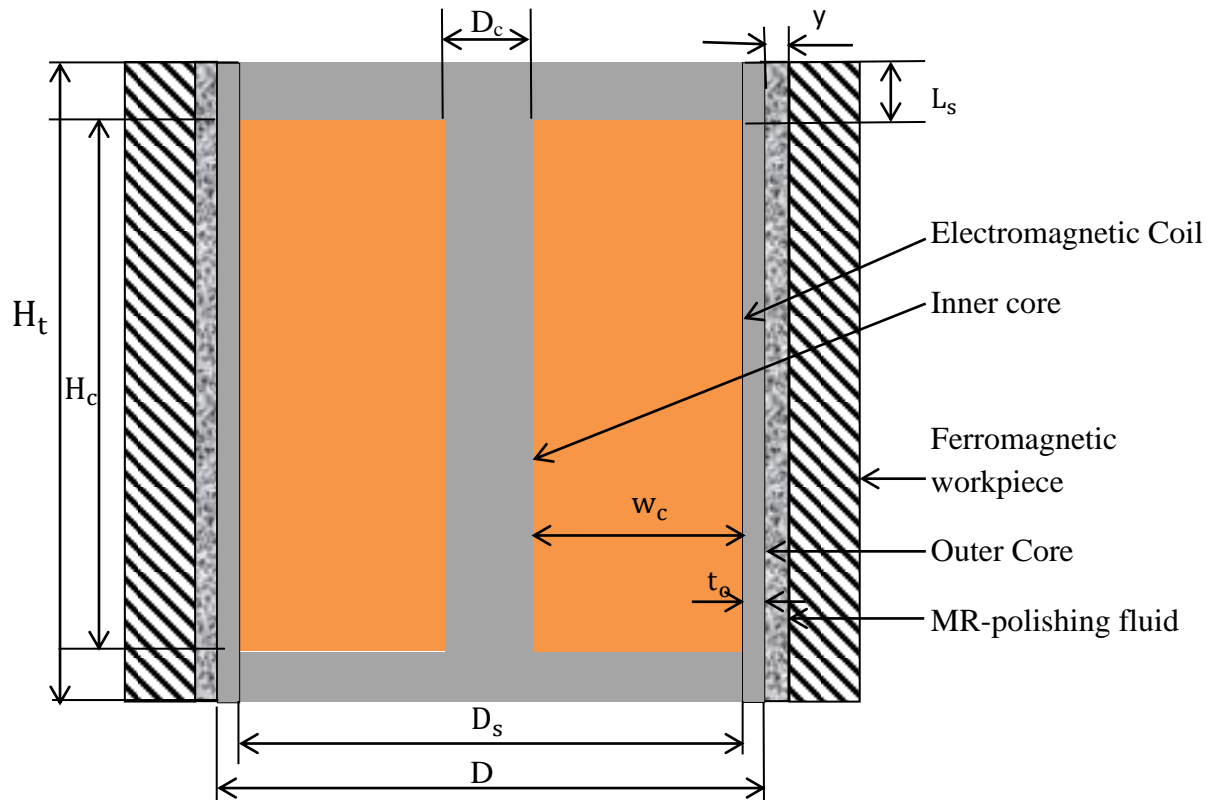


Figure 3.3: Schematic diagram of MRH tool retained stiffen MR polishing fluid

- Where,
- w_c = width of coil
 - D_s = diameter of spool
 - D_c = diameter of central part of inner core
 - D = outer diameter of tool over which MRP-fluid will flow
 - H_c = height of central inner part of core
 - H_t = total height of the MRH tool
 - t_o = thickness of outer surface of MRH tool
 - y = thickness of MR polishing fluid

3.2.2 Electromagnet Model of MRH tool in Maxwell ANSOFT V13 Software

A 3-dimensional model of MR finishing tool with ferromagnetic workpiece is made in Maxwell ANSOFT V13 software. Firstly a core is made as shown in Fig.3.1 with some

arbitrary dimensions. Core is made up of iron with relative permeability 600. Over the inner core of MRH tool an electromagnet coil is wound which is made up of copper wire size 1 mm as shown in Fig.3.2. Then outer part of the core is made over the core and electromagnetic coil as shown in Fig. 3.3. In the presence of magnetic field MR polishing fluid gets stiff over the outer core of MRH tool, stick to the outer part of the core and perform the finishing of internal surface of the workpiece as shown in Fig. 3.3. The material selected for electromagnet coil is copper of relative permeability 1. Number of turns and current is assigned to the electromagnetic coil. Number of turns for electromagnetic coil is calculated and assigned on the basis of tool dimensions.

$$\text{Number of copper wire turns of electromagnetic coil} = W_c \times H_c \quad (3.1)$$

Over the MR polishing fluid ferromagnetic workpiece is made with a constant thickness of 8 mm. Thickness of workpiece is taken constant because for all the cases of FE analysis there will be similarity of surface to be finished. Electromagnet copper wire diameter is assumed as 1 mm (20 SWG).

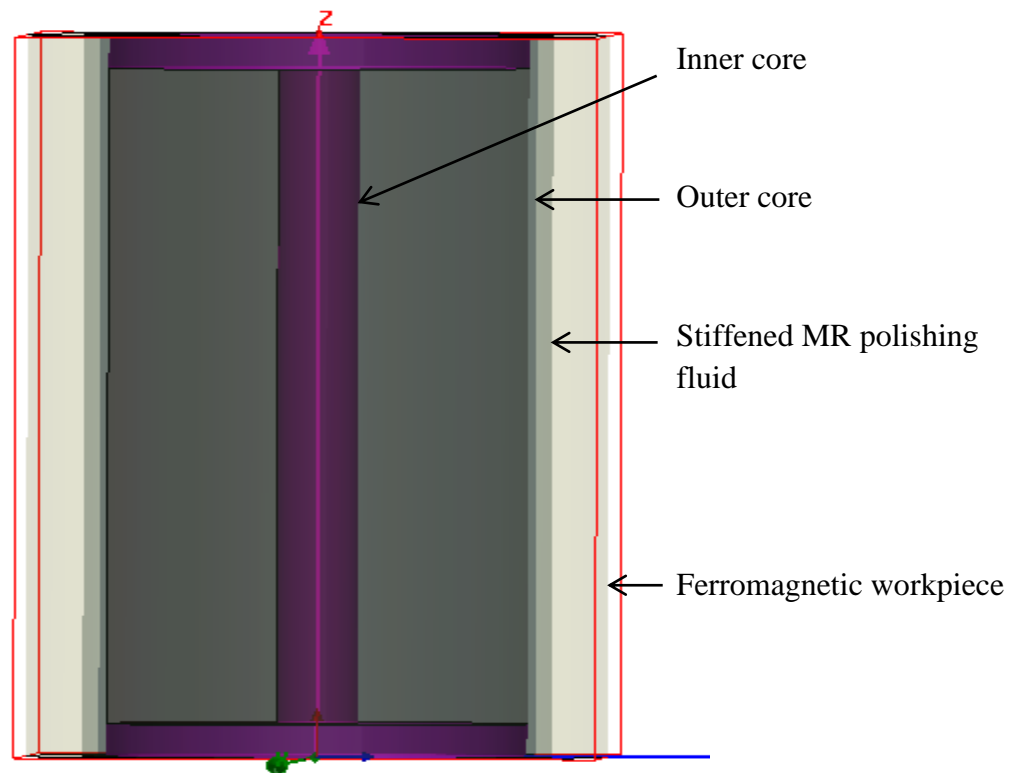


Figure 3.4: Electromagnet Model of Magnetorheological Honing (MRH) Tool

The relative permeability of MR polishing fluid material is given as 5. A 3-dimensional electromagnet model of MRH tool with workpiece surface has been made using Maxwell

ANSOFT V13 software as shown in Fig. 3.4. Detail of assigned specifications to the 3D electromagnet model is given in Table 3.1 Its dimensions are decided by performing simulation for various cases.

3.2.3 Finite Element (FE) Analysis of MRH tool along with Ferromagnetic Workpiece Surface for Magnetic Flux Density

Developed electromagnet model in Maxwell ANSOFT V13 software is simulated and magnetic flux density distribution is observed as shown in Fig 3.5. Main aim of performing simulations is to find out the condition for which we get maximum magnetic field and force on the workpiece. Initially FE simulation is performed with an arbitrary dimension and then later on changes are made step-by-step according to the FE simulation results.

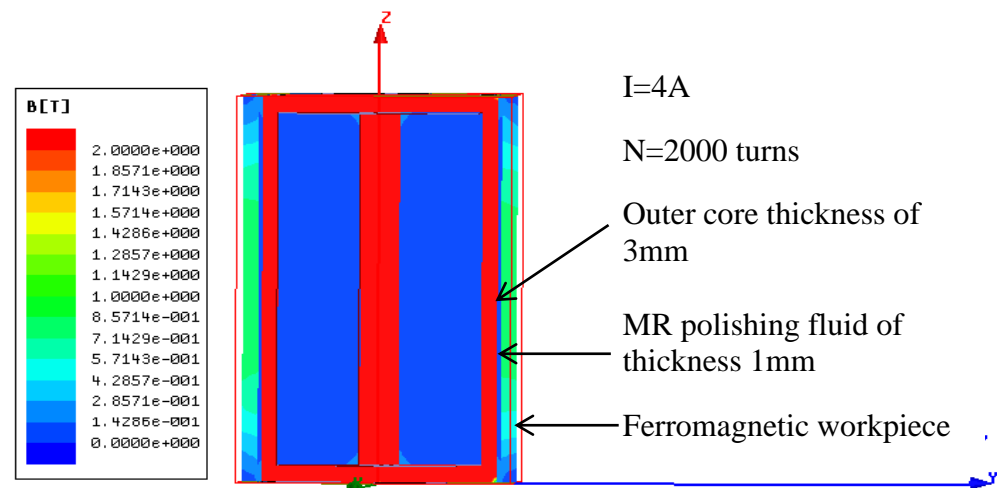


Figure 3.5: Magnetic flux density distribution in MRH tool with ferromagnetic workpiece

The magnetostatic FE analysis of MRH tool with workpiece is done using Maxwell ANSOFT V13 software shown in Fig.3.5. to observe the value of magnetic flux density at different locations of MRH finishing tool. Here dimensions are taken arbitrary. Main motive is to explain the FE analysis result of MRH tool with ferromagnetic workpiece. The magnetic flux density distribution at different locations of tool and workpiece is shown in Fig.3.5. The MRH tool with ferromagnetic workpiece is designed with outer core thickness of 3mm and working gap for MR polishing fluid is taken to be 1mm. Maximum Magnetic flux density value is obtained on the outer core. Value of magnetic flux density in MR polishing fluid is less as compared to the outer surface of MRH tool. Due to the maximum flux density

gradient on outer surface of MRH tool, MR polishing fluid gets stick to the outer periphery of MRH tool. Magnitude of magnetic flux density is low on the surface of workpiece, so non-ferromagnetic abrasives go to the workpiece surface. Due to the rotatory action of MRH tool, abrasives of surface of workpiece perform finishing operation.

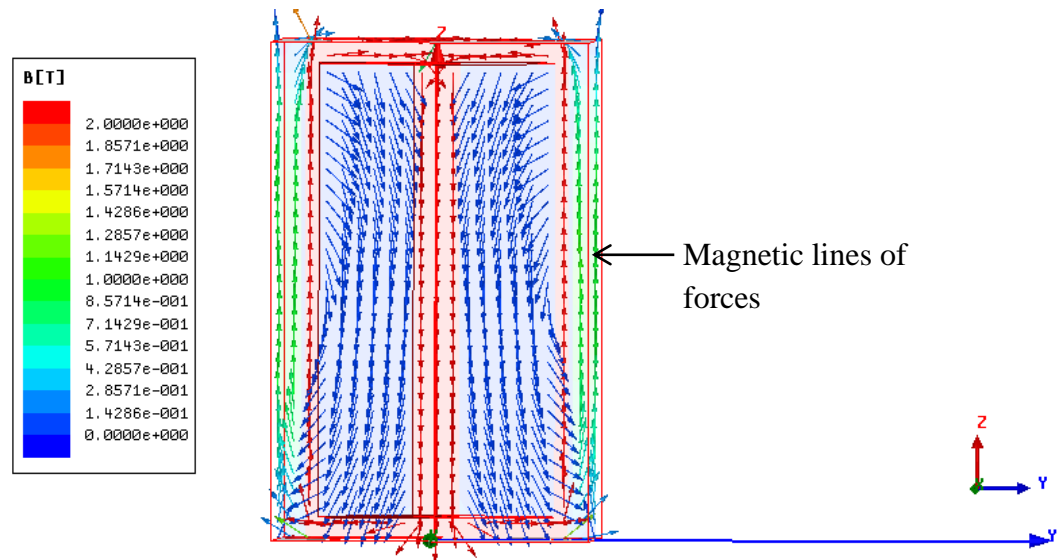
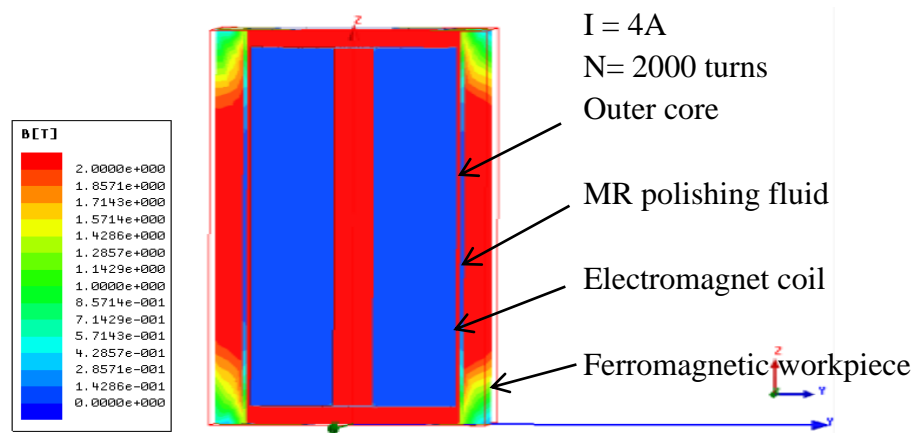


Figure 3.6: Magnetic Lines of forces direction in FE analysis of MRH tool

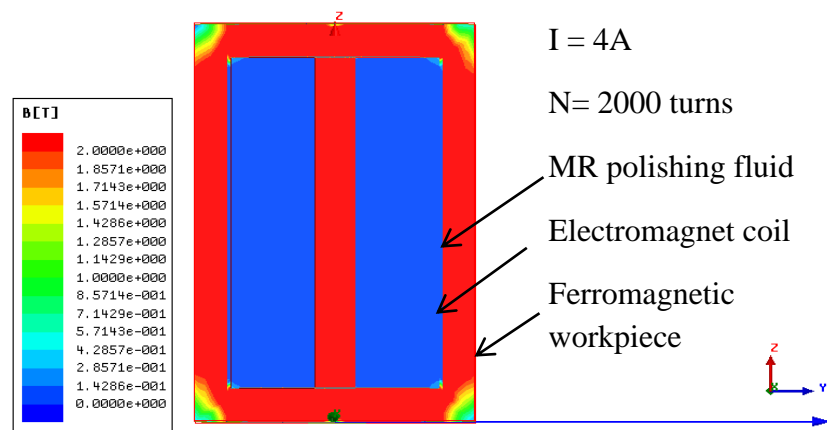
In Figure 3.6 direction of magnetic lines of force is shown. Magnetic line of forces originates from inner core, flow outwards from the bottom of the core into the workpiece and then come inside the from the upper part of inner core. Intensity of magnetic line of forces is more at inner part of the core and these magnetic lines of forces emerge out from the central bottom part of the core and move through MR polishing fluid and workpiece. The intensity of magnetic line of forces gets week as it passes though the workpiece.

3.2.4 Optimizing the Tool Dimensions on basis of FE simulation results.

Initially tool is modeled without outer core with $D_s = 52$ mm, $D_c = 10$ mm, $L_s = 10$ mm, $H_c = 100$ mm and simulation is performed as shown in Fig. 3.7 (a). Thickness of workpiece is taken constant i.e. 7 mm for all the cases .Then tool is modeled and simulated with same parameters but with including outer core of thickness 1 mm in Fig. 3.7 (b) and comparison is done as shown in Fig.3.7 (a) and 3.7 (b).



(a)



(b)

Figure 3.7: Magnetic flux density distribution in MRH tool (a) with outer core (b) without outer core

Here MR polishing fluid spacing is taken to be 1mm for both the cases. In Fig.3.7. (a) MRH tool with ferromagnetic workpiece is magneto statically simulated with outer core with thickness 1 mm and in Fig.3.7. (b) there is no outer core. It can be clearly observed by comparing Fig.3.7. (a) and Fig.3.7.(b) that there is an appreciable increase in magnetic field in MR-polishing fluid region by including outer core over the tool. From this it is concluded that there should be an outer core film over the tool to get better magnetic field in MR polishing fluid region.

Now MRH tool with ferromagnetic workpiece is magneto statically simulated and changes are made one-by-one for getting maximum flux density. Different cases considered for designing the tool are in this way:-

- (a) FE Analysis by varying MR polishing fluid thickness
- (b) FE Analysis by varying outer core thickness
- (c) FE Analysis by varying spool thickness
- (d) FE Analysis by varying the electromagnet current
- (e) FE Analysis by varying the inner core diameter
- (f) FE Analysis by varying diameter of the inner core with changing the number of turns of coil accordingly
- (g) FE Analysis by varying height of inner core, H_c
- (h) FE Analysis by varying height of the inner core, H_c while keeping the number of turns of coil constant

(a) FE Analysis by varying MR polishing fluid thickness and keeping outer core thickness constant i.e. 1 mm

MRH tool with ferromagnetic workpiece is modeled and simulated by taking $D_s = 52$ mm, $D_c = 10$ mm, $L_s = 10$ mm and $H_c = 100$ mm. Outer core thickness is taken fixed as 1 mm and MR polishing fluid is varied from 1 mm to 5 mm and comparison is done as shown in Fig.3.8. Current given to the coil is taken to be $I = 4$ A and number of turns of coil, $N = 2000$ turns. By comparing FE magneto static simulation results of MRH tool in Fig.3.8.(a), (b), (c), (d) and (e), it has been seen that maximum magnetic flux density is obtained when MR polishing fluid thickness is kept as 1mm.. Also it can be seen that as the thickness of MR polishing fluid reduces, magnitude of magnetic flux density increases on outer surface of the MRH tool. The more magnetic flux density on outer surface of MRH tool, the more is the MR polishing fluid retain and become stiff which is required for finishing action. Therefore MR polishing fluid of 1 mm thickness can produce better surface finish on workpiece surface.

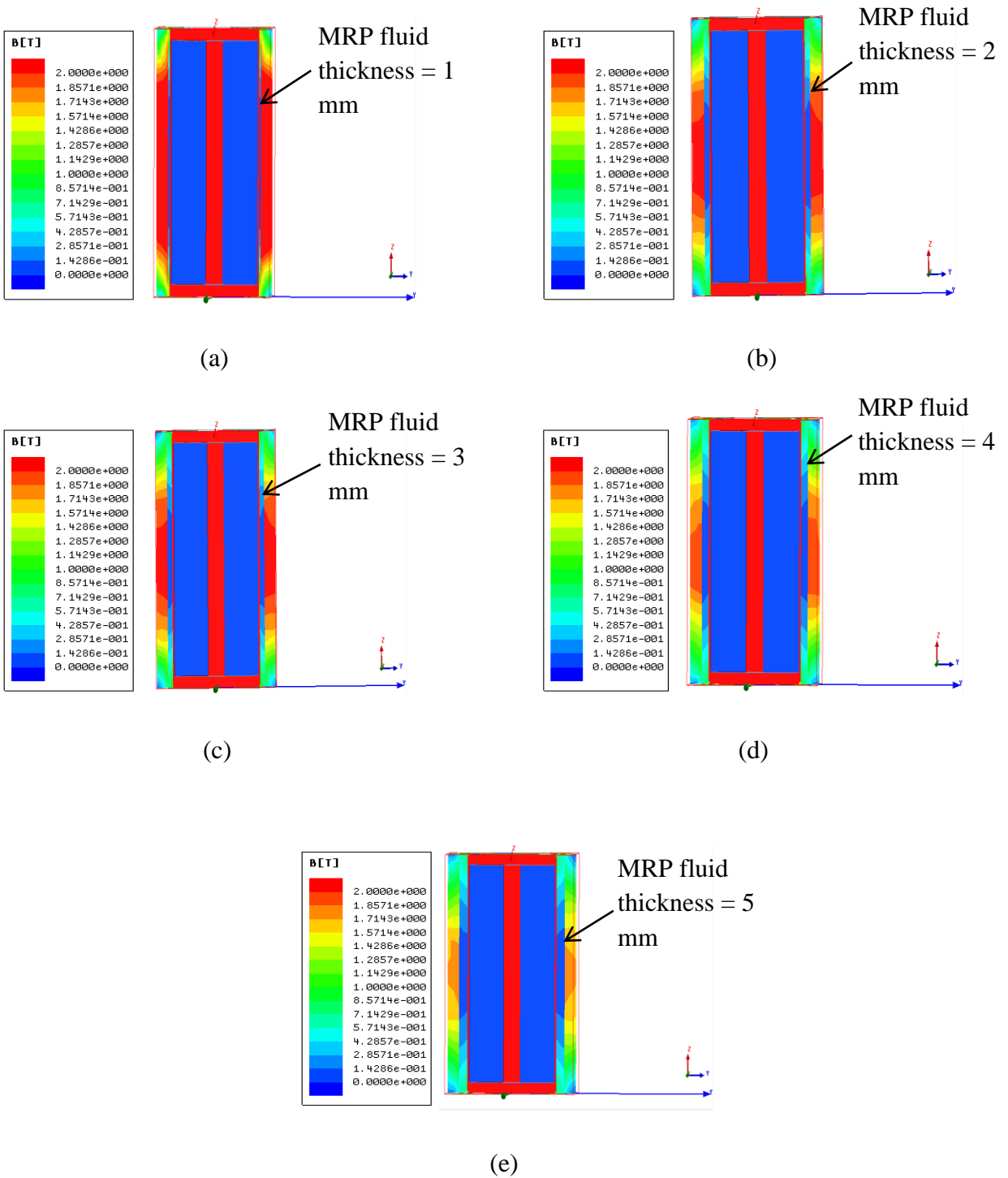


Figure 3.8: Magnetic flux density distribution of MRH tool for ferromagnetic workpiece surface when MR polishing fluid thickness (a) 1 mm (b) 2 mm (c) 3 mm (d) 4 mm and (e) 5mm

(b)FE Analysis by varying outer core thickness and keeping MR polishing fluid thickness constant i.e. 1 mm

MRH tool with ferromagnetic workpiece is modeled and simulated by taking $D_s = 52$ mm, $D_c = 10$ mm, $L_s = 5$ mm and $H_c = 100$ mm.

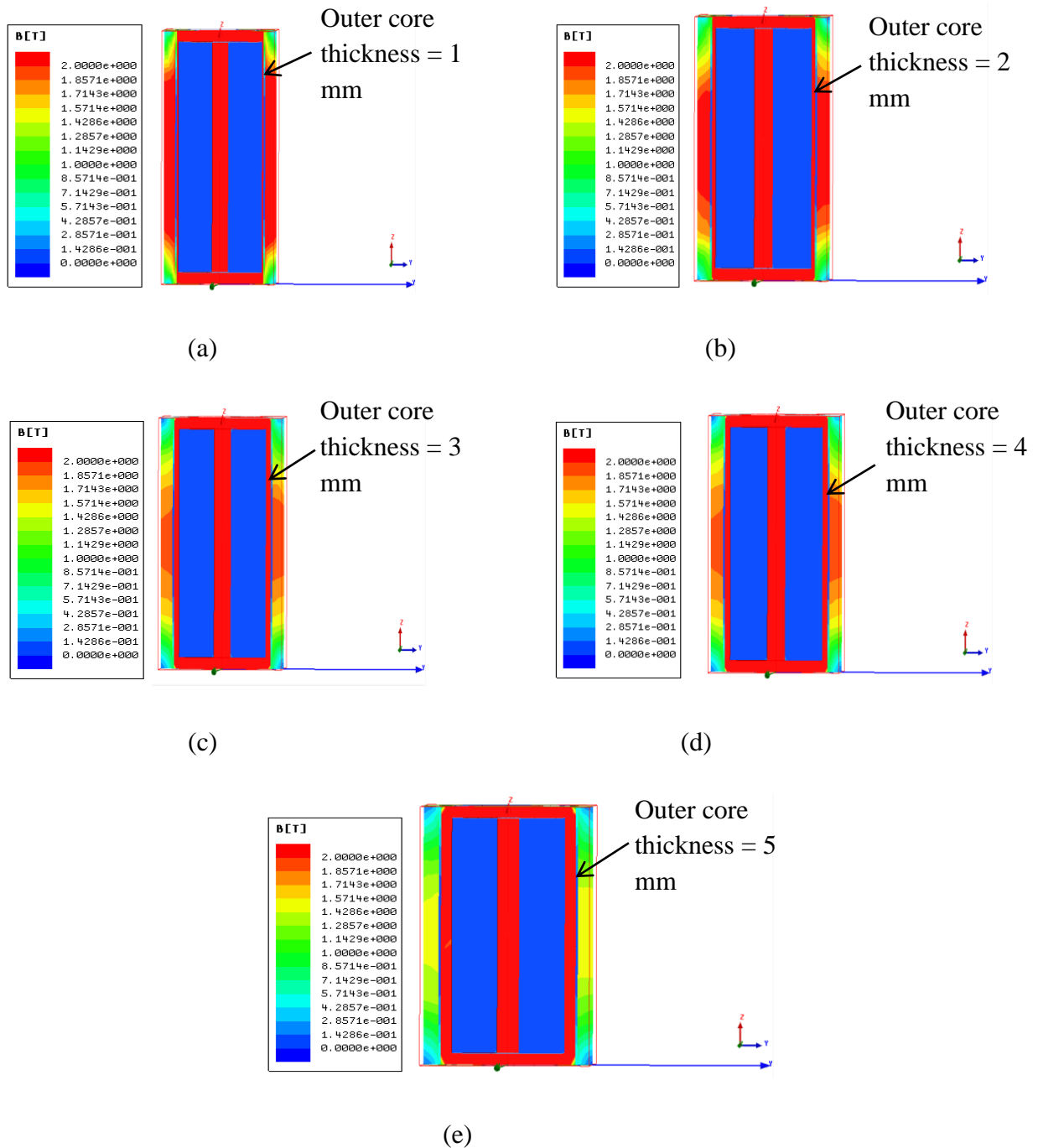


Figure 3.9: Magnetic flux density distribution of MRH tool for ferromagnetic workpiece surface when outer core thickness (a) 1 mm (b) 2 mm (c) 3 mm (d) 4 mm and (e) 5mm

MR polishing fluid thickness is taken fixed as 1 mm and outer core thickness is varied from 1 mm to 5 mm and comparison is done as shown in Fig.3.9. Current given to the coil is taken to be $I=4$ A and number of turns of coil, $N = 2000$ turns. By comparing FE magneto static simulation results of MRH tool in Fig.3.9 (a), (b), (c), (d) and (e), it has been seen that maximum magnetic flux density is obtained when outer thickness is kept as 1mm. Also it can be observed that as the thickness of outer core reduces, magnetic flux density increases on the outer surface of the MRH tool. The more magnetic flux density on outer surface of MRH tool, more is the MR polishing fluid retained and stiffen which is required for finishing action. Therefore outer core of 1 mm thickness can produce better surface finish on workpiece surface.

(c) FE Analysis by varying the spool thickness

MRH tool with ferromagnetic workpiece is modeled and simulated by taking $D_s= 52$ mm, $D_c = 10$ mm, and $H_c = 100$ mm. MR polishing fluid and outer core thickness is taken fixed as 1 mm. Thickness of spool L_s is varied from 1 mm to 5 mm and comparison is done as shown in Fig.3.10. (a), (b), (c), (d) and (e). Current given to electromagnet coil is $I=4$ A and number of turns of electromagnet coil, $N = 2000$ turns. By comparing FE magneto static simulation results of MRH tool in Fig.3.10.(a), (b), (c), (d) and (e) it has been seen that there is no change in magnetic flux density is obtained when spool thickness is changed. Any value of spool thickness can be taken for optimizing the tool Therefore spool of 5 mm thickness is taken for design of MRH tool so that tool become neither too large nor too small.

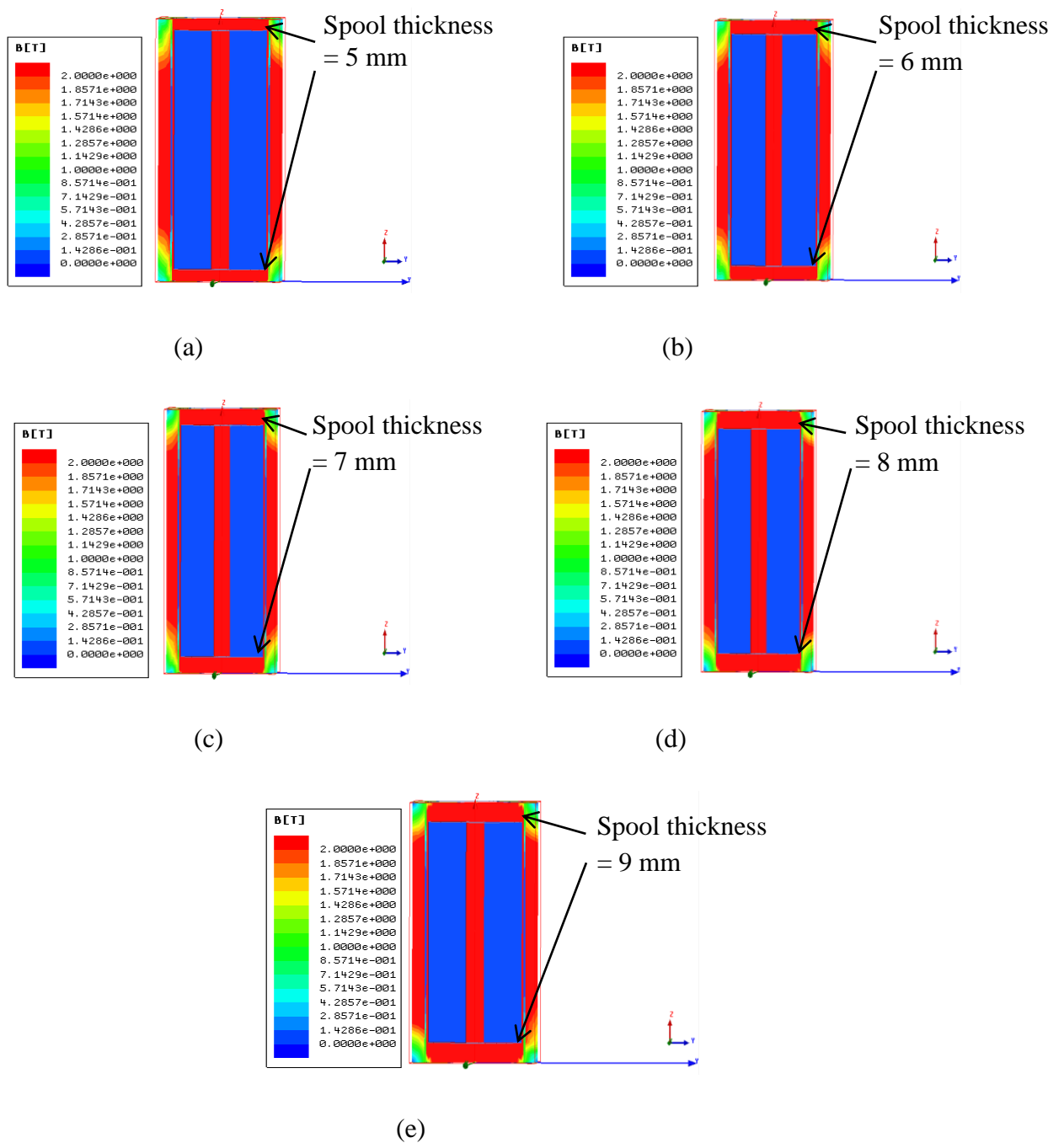
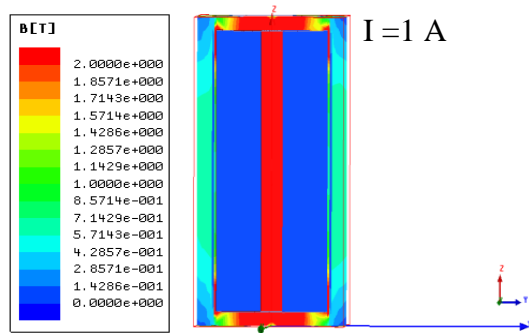
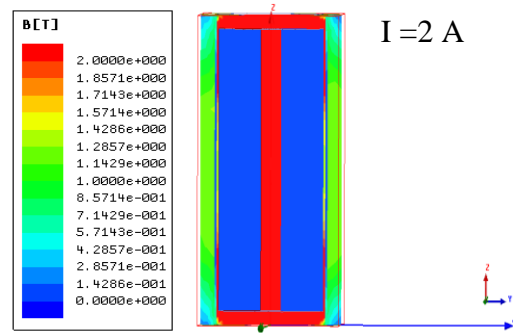


Figure 3.10: Magnetic flux density distribution of MRH tool for ferromagnetic workpiece surface when spool thickness (a) 1 mm (b) 2 mm (c) 3 mm (d) 4 mm and (e) 5mm

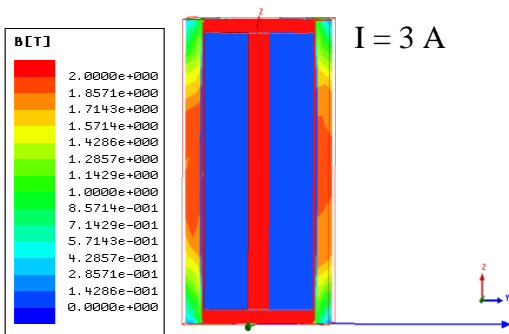
(d) FE Analysis by varying the electromagnet current



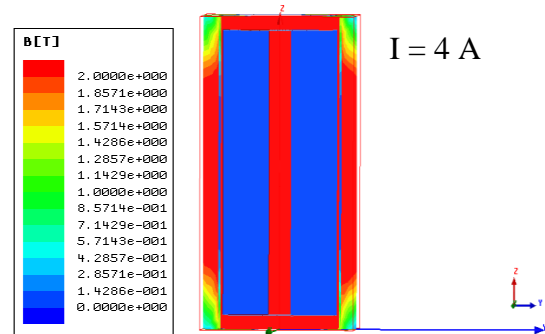
(a)



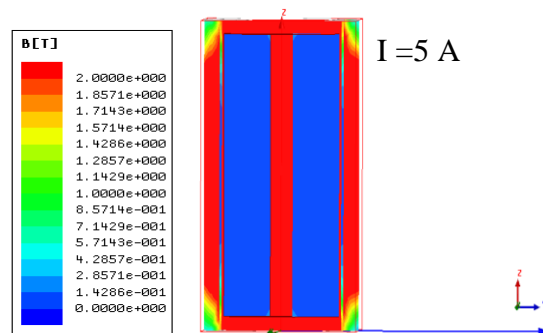
(b)



(c)



(d)



(e)

Figure 3.11: Magnetic flux density distribution of MRH tool for ferromagnetic workpiece surface when current given to electromagnet coil (a) 1 A (b) 2A (c) 3 A (d) 4 A and (e) 5 A

MRH tool with ferromagnetic workpiece is modeled and simulated by taking $D_s = 52$ mm, $D_c = 10$ mm, $L_s = 5$ mm and $H_c = 100$ mm. Outer core and MR polishing fluid thickness is taken as 1 mm and current given to the electromagnet coil is varied from 1A to 5A and comparison is done as shown in Fig. 3.11.(a), (b), (c), (d) and (e). Number of turns of coil, $N = 2000$ turns. By comparing FE magneto static simulation results of MRH tool in Fig.3.11.(a), (b), (c), (d) and (e), it has been seen that value of maximum magnetic flux density is obtained when current given to the electromagnet coil as 5 A. Also it can be seen that as the current given to the electromagnet coil increases, value of magnetic flux density increases on outer surface of the MRH tool. The more magnetic flux density on outer surface of MRH tool, more is the MR polishing fluid retained and stiffen which is required for finishing action. Therefore current of 5 A given to electromagnet coil can produce better surface finish on workpiece surface.

(e) FE Analysis by varying the inner core diameter keeping number of turns of coil to be constant

MRH tool with ferromagnetic workpiece is modeled and simulated by taking $D_s = 52$ mm, $L_s = 5$ mm and $H_c = 100$ mm. Outer core and MR polishing fluid thickness is taken fixed as 1 mm. Diameter of core D_c is changed from 10 mm to 6 mm and number of turns of coil N is kept constant i.e. 2000 for 5 cases. Current given to the coil $I = 4$ A and comparison is done as shown in Fig.3.12 (a), (b), (c), (d) and (e). By comparing FE magneto static simulation results of MRH tool in Fig.3.12 (a), (b), (c), (d) and (e), it has been seen that magnetic flux density on outer core and workpiece goes on decreasing with decrease in diameter of inner core even when number of turns of coil N is constant. Also it can be seen that as diameter of inner core decreases (number of turns of electromagnet coil is constant), value of magnetic flux density decreases on the outer surface of the MRH tool. The more magnetic flux density on outer surface of MRH tool more is the MR polishing fluid retain and stiff which is required for finishing action. Therefore suitable value for diameter of inner core is finalized as 10 mm so that tool becomes neither too small nor too large and can produce better surface finish on workpiece surface.

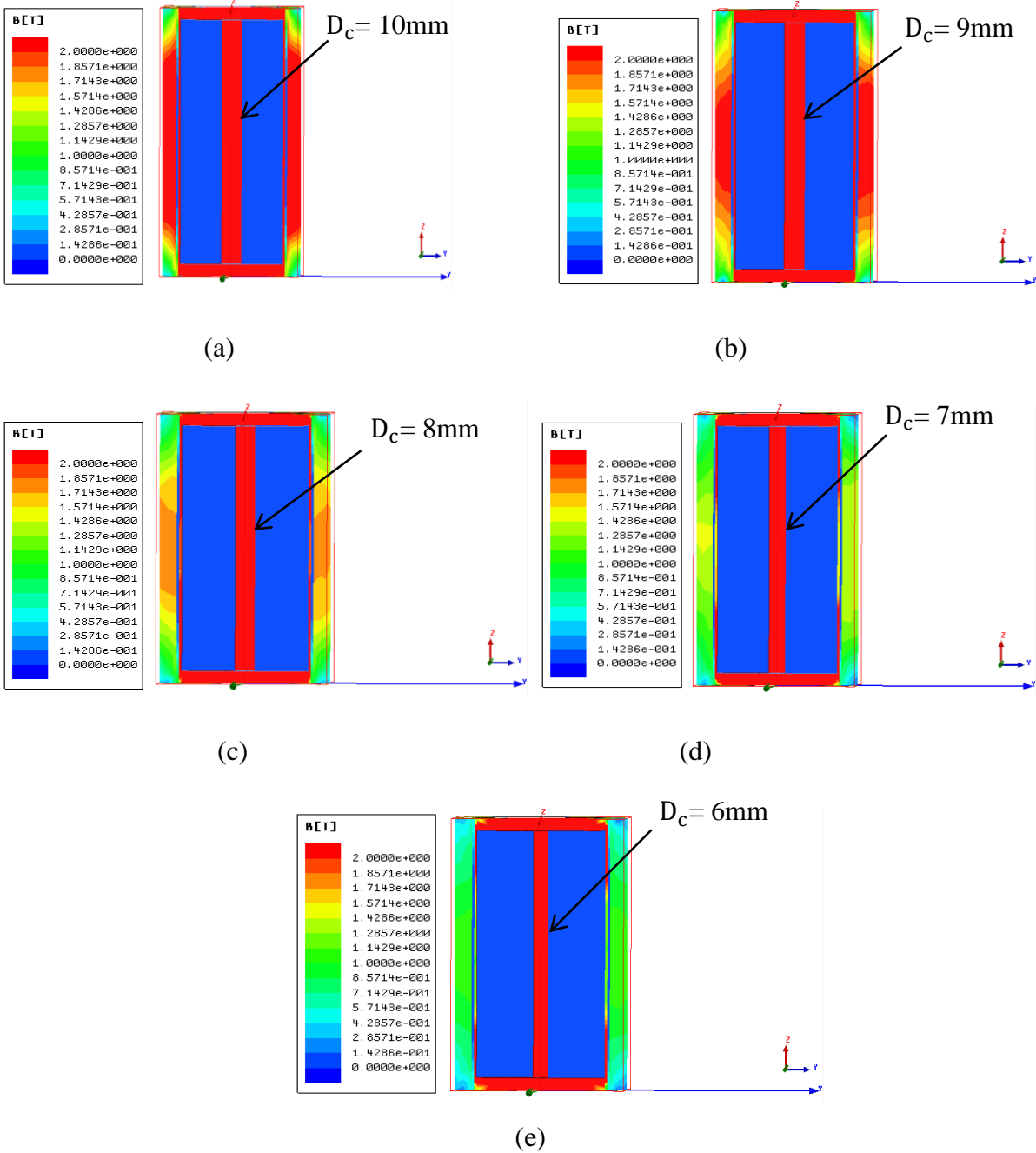


Figure 3.12: Magnetic flux density distribution of MRH tool for ferromagnetic workpiece surface when diameter of inner core D_c as (a) 10mm (b) 9mm (c) 8mm (d) 7mm (e) 6mm

(f) FE Analysis by varying diameter of the inner core with changing the number of turns of coil accordingly

MRH tool with ferromagnetic workpiece is modeled and simulated by taking $D_s = 52$ mm, $L_s = 5$ mm and $H_c = 100$ mm. Outer core and MR polishing fluid thickness is taken fixed as 1 mm.

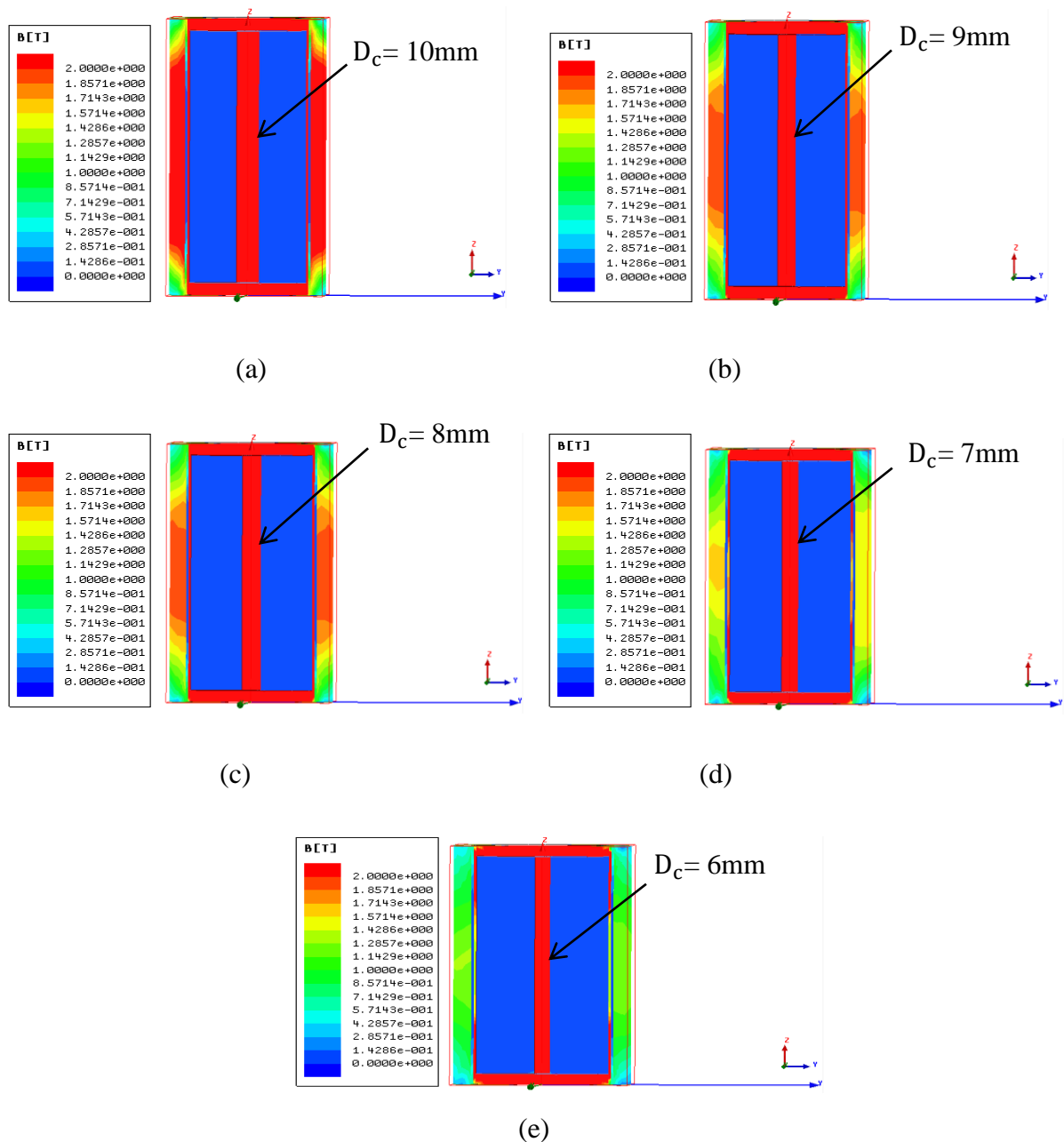


Figure 3.13: Magnetic flux density distribution of MRH tool for ferromagnetic workpiece surface when diameter of inner core D_c is changing (number of turns of electromagnet coil changes accordingly) as (a) 10mm (b) 9mm (c) 8mm (d) 7mm (e) 6mm

Diameter of core D_c is changed from 10 mm to 6 mm and number of turns of electromagnet coil is changed accordingly with dimensions as illustrated in equation 3.1. Current given to the coil $I = 4A$ and comparison is done as shown in Fig.3.13 (a), (b), (c), (d) and (e). By comparing FE magneto static simulation results of MRH tool in Fig.3.13 (a), (b), (c), (d) and (e), it has been seen that magnetic flux density on outer core and workpiece goes on decreasing with descending diameter of inner core. Also it can be seen that as diameter of inner core decreases (number of turns of electromagnet coil is changes accordingly), value magnetic flux density decreases on the outer surface of the MRH tool. The more magnetic flux density on outer surface of MRH tool, more is the MR polishing fluid retained and stiffen which is required for finishing action. Therefore suitable value for diameter of inner core is finalized as 10 mm so that tool becomes neither too small nor too large and can produce better surface finish on workpiece surface.

(g) FE Analysis by varying height of the core, H_c

MRH tool with ferromagnetic workpiece is modeled and simulated by taking $D_s = 52$ mm, $D_c = 10$ mm, $L_s = 5$ mm. Outer core and MR polishing fluid thickness is taken fixed as 1 mm. Height of core H_c is varied from 100 mm to 60 mm. Number of turns of coil N is variable for different cases and is calculated by equation 3.1. Current given to the coil $I = 4A$ and comparison is done as shown in Fig.3.14. (a), (b), (c), (d) and (e). By comparing FE magneto static simulation results of MRH tool in Fig.3.14. (a), (b), (c), (d) and (e), it has been seen that there is no appreciable change in magnetic field as height of the tool goes on decreasing. It is difficult to handle the motion (rotating and reciprocating) to a long tool. So, suitable value for height of the tool is finalized to be 60 mm so that tool becomes neither too small nor too large. Current given to the coil is 4 A.

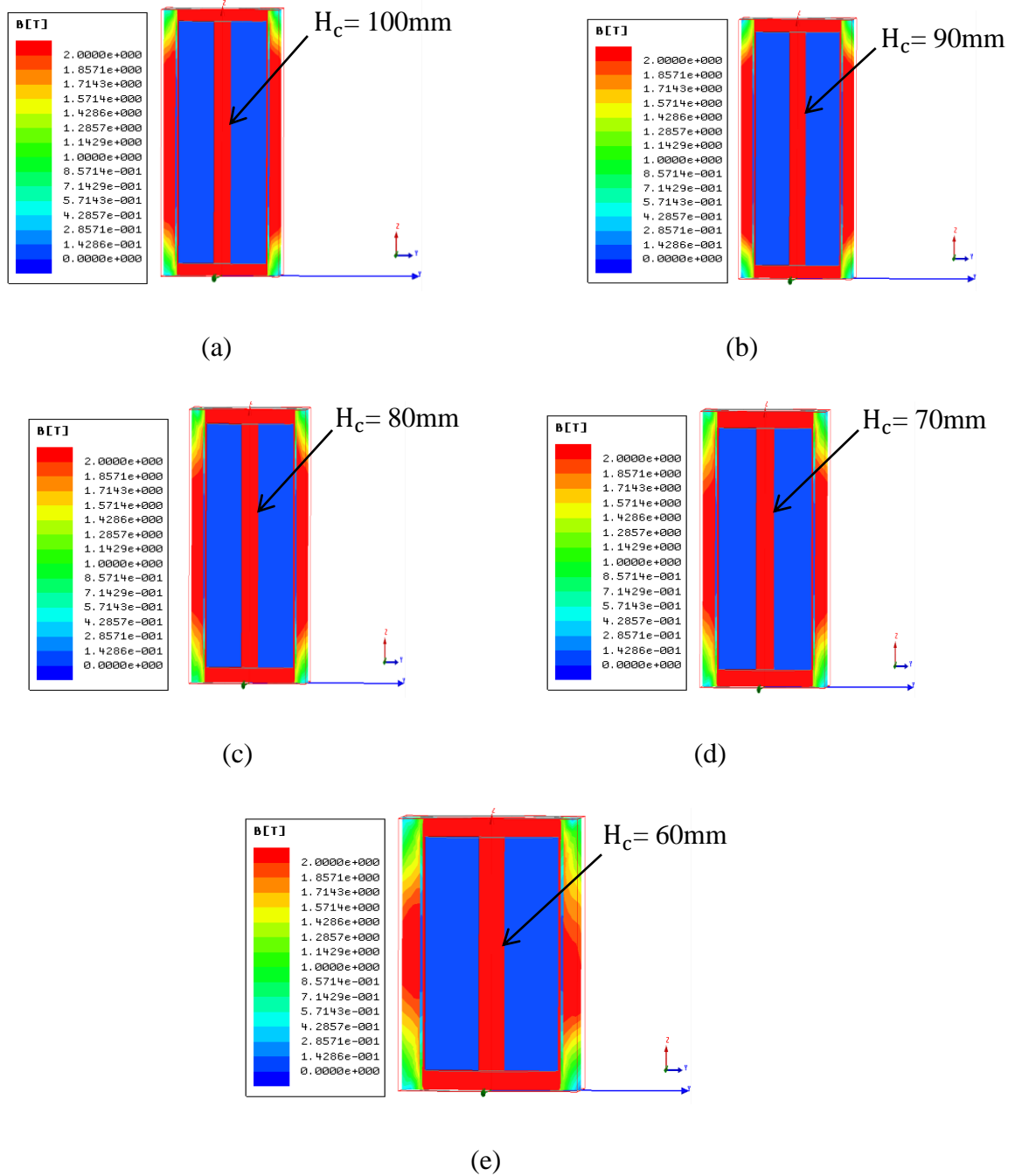


Figure 3.14: Magnetic flux density distribution of MRH tool for ferromagnetic workpiece surface when height of inner core H_c (a) 100mm (b) 90mm (c) 80mm (d) 70mm (e) 60mm

(h) FE Analysis by varying height of the core, H_c while keeping the number of turns of coil constant

MRH tool with ferromagnetic workpiece is modeled and simulated by taking $D_s = 52$ mm, $D_c = 10$ mm, $L_s = 5$ mm. Outer core and MR polishing fluid thickness is taken fixed as 1 mm. Height of core H_c is varied from 100 mm to 60 mm but in this case number of turns of coil N is kept constant i.e. 2000 for different cases. It is done by increasing width of the tool accordingly. Current given to the coil $I = 4$ A and comparison is done as shown in Fig.3.15 (a), (b), (c), (d) and (e). By comparing FE magneto static simulation results of MRH tool in Fig.3.15 (a), (b), (c), (d) and (e), it has been seen that there is no appreciable change in magnetic field with changing height of the tool goes on decreasing even number of turns of coil is constant. So, suitable value for height of the tool is finalized to be 60 mm so that tool becomes neither too small nor too large. Number of turns of coil is given according to height of the coil H_c as explained in equation 3.1. Current given to the coil is 4 A.

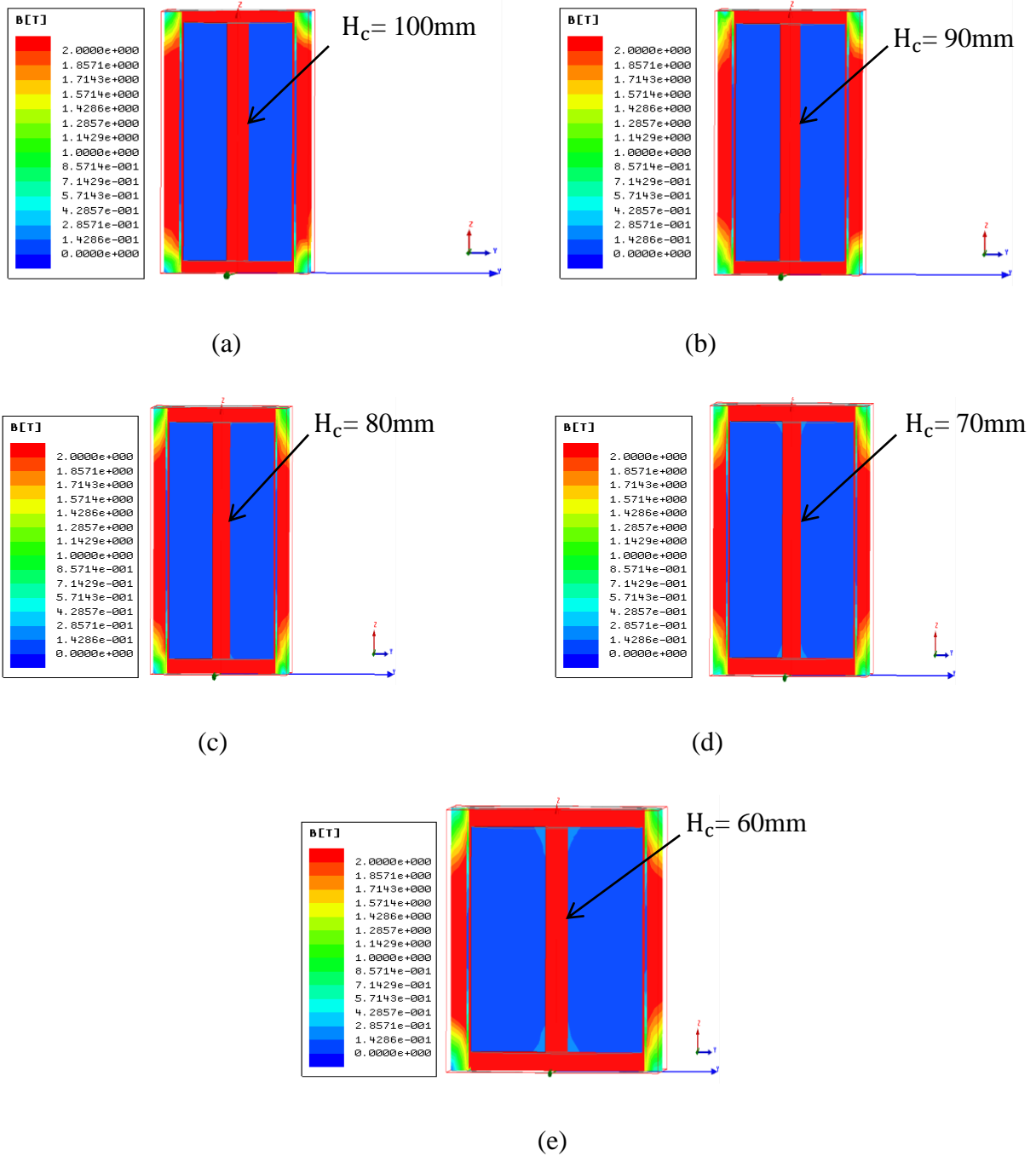


Figure 3.15: Magnetic flux density distribution of MRH tool for ferromagnetic workpiece surface when number of turns of coil kept constant and varying height of core H_c as (a) 100mm (b) 90mm (c) 80mm (d) 70mm (e) 60mm

3.2.5 Obtained Optimum Dimensions of MRH tool from Maximum Flux Density Distribution Gradient from FE Analysis

MRH tool is modeled and simulated in Maxwell ANSOFT V13 software. From the FE simulation results tool dimensions have been optimized. The main aim of optimizing the tool is to get the situation in which maximum magnetic field on outer surface of MRH tool is obtained. MRH tool dimensions obtained from FE simulation results are in this way:

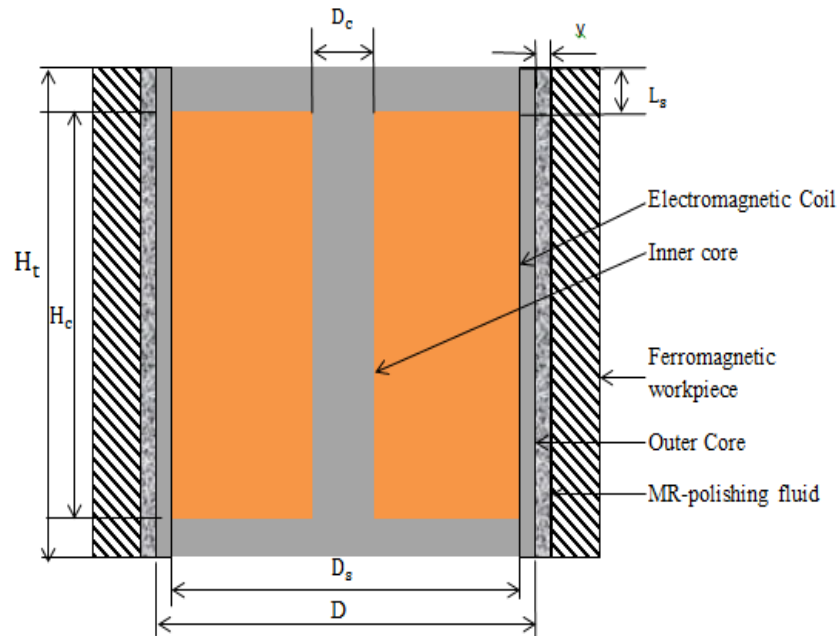


Figure 3.16: Schematic diagram of MRH tool with ferromagnetic workpiece

Table 3.2: Optimum dimensions of MRH Tool obtained from FE simulation of MRH tool with ferromagnetic workpiece

Parameters of MRH Tool	Optimum Value
Height of central inner part of core (mm) H_c	60 mm
Total height of the tool (mm) H_t	72 mm
Radius of central part of inner core (mm) R_c	5 mm
Outer diameter of tool over which MRP-fluid will flow (mm) D	54 mm
Diameter of spool (mm) D_s	52 mm
Thickness of spool L_s	6 mm
MR polishing fluid thickness y	1 mm

3.3 FE Analysis for Magnetic Flux Density Distribution in a Cycle of Finishing Operation

MRH tool reciprocates up and down inside the cylindrical workpiece as shown in 3.17. Finite element analysis of MRH tool with ferromagnetic workpiece during the reciprocation of MRH tool at different positions is shown in Fig. 3.18 to Fig.3.25. MRH tool enters the ferromagnetic workpiece and moves downward in Fig. 3.18 to Fig. 3.20, it enters completely inside ferromagnetic workpiece in Fig. 3.21 and then comes out of the ferromagnetic workpiece in Fig. 3.22 to Fig. 3.25. Then MRH tool moves up in same manner concentric with ferromagnetic workpiece. It repeats the cycle again and again to perform the finishing action.

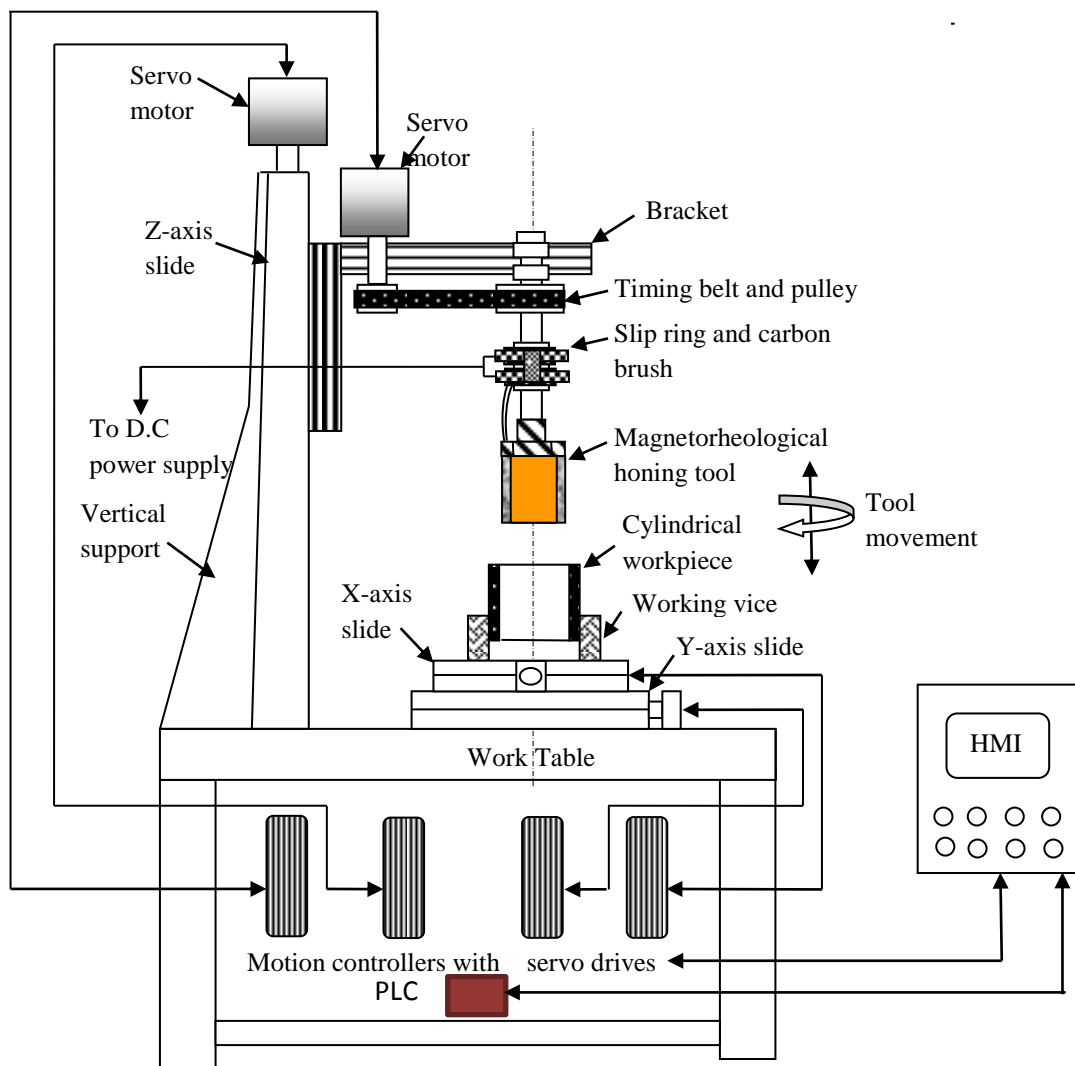


Figure 3.17: Schematic diagram of Novel Magnetorheological Honing Setup

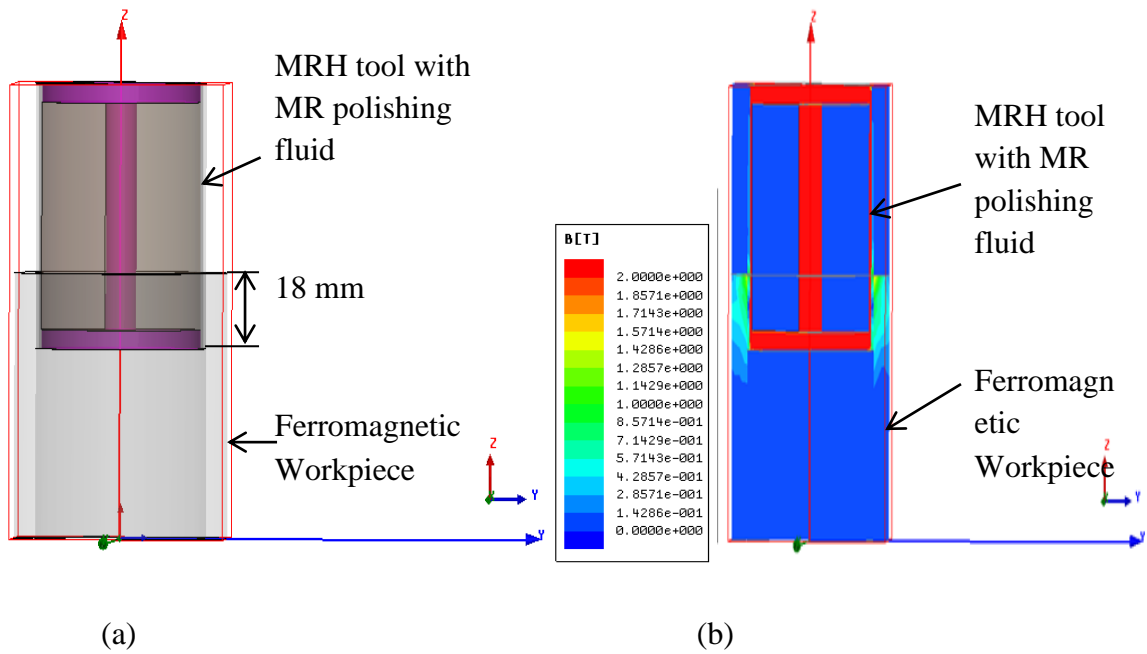


Figure 3.18: MRH tool for ferromagnetic workpiece when base of lower spool is 18mm below from top of the ferromagnetic workpiece (a) Electromagnet model (b) Magnetic flux density distribution

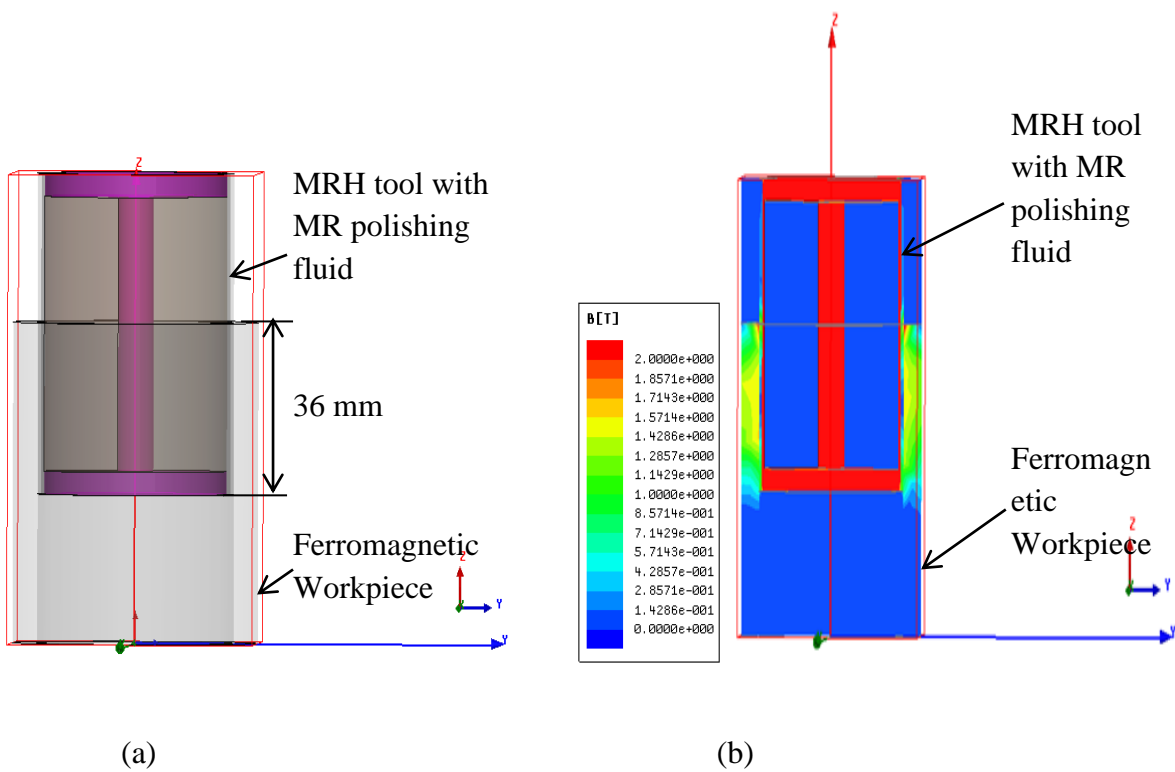


Figure 3.19: MRH tool for ferromagnetic workpiece when base of lower spool is 36mm below from top of the ferromagnetic workpiece (a) Electromagnet model (b) Magnetic flux density distribution

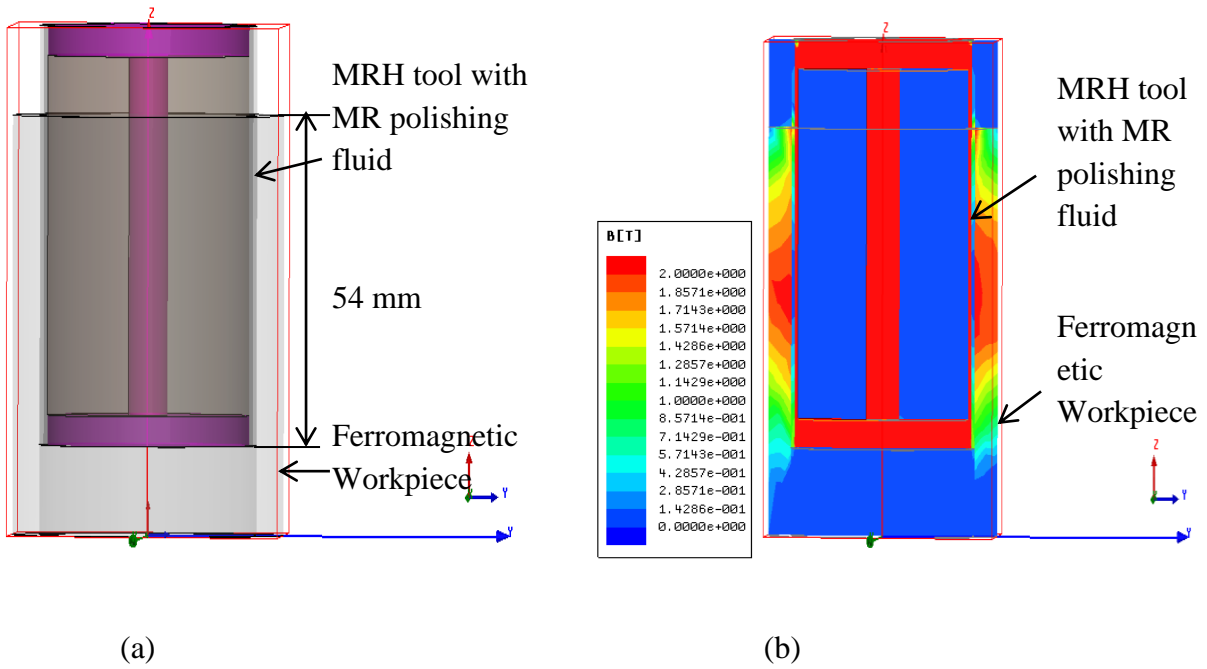


Figure 3.20: MRH tool for ferromagnetic workpiece when base of lower spool is 54 mm below from top of the ferromagnetic workpiece (a) Electromagnet model (b) Magnetic flux density distribution

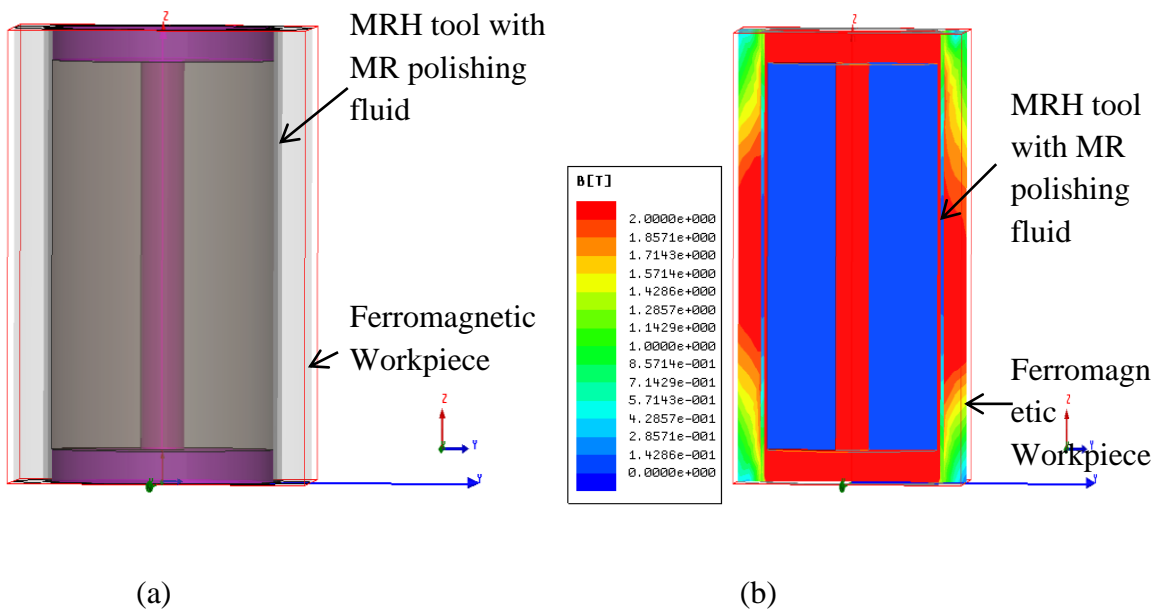


Figure 3.21: MRH tool for ferromagnetic workpiece when base of MRH tool is concentric with workpiece (a) Electromagnet model (b) Magnetic flux density distribution

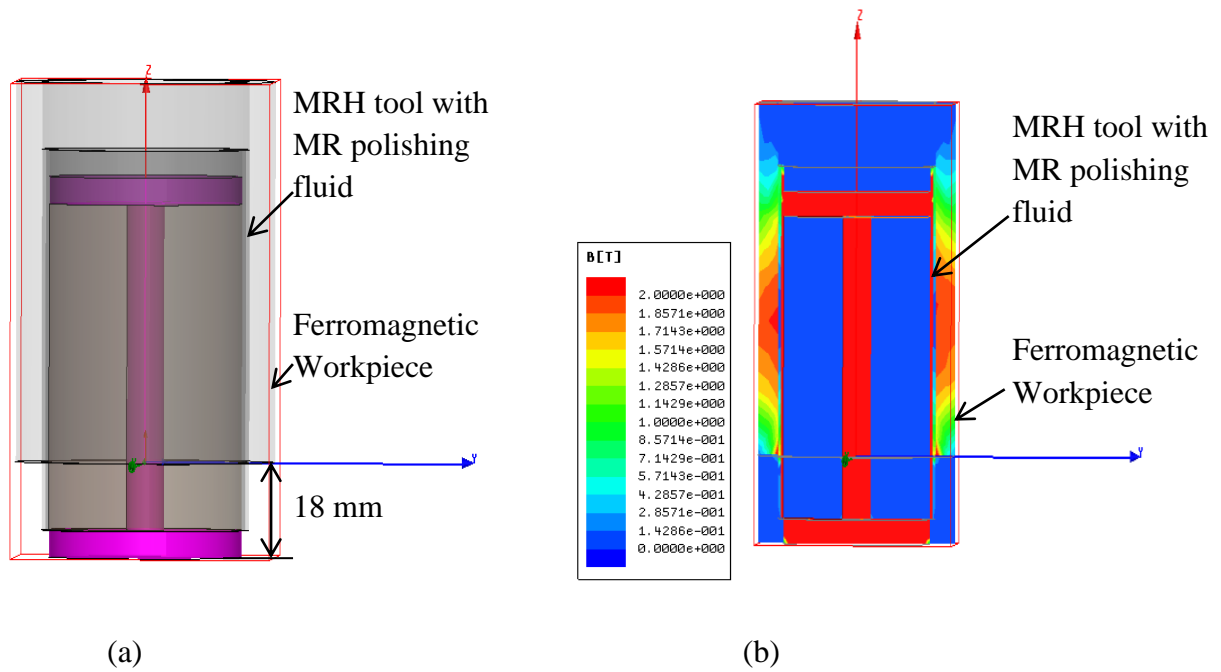


Figure 3.22: MRH tool for ferromagnetic workpiece when base of lower spool is 18 mm below from bottom of the ferromagnetic workpiece (a) Electromagnet model (b) Magnetic flux density distribution

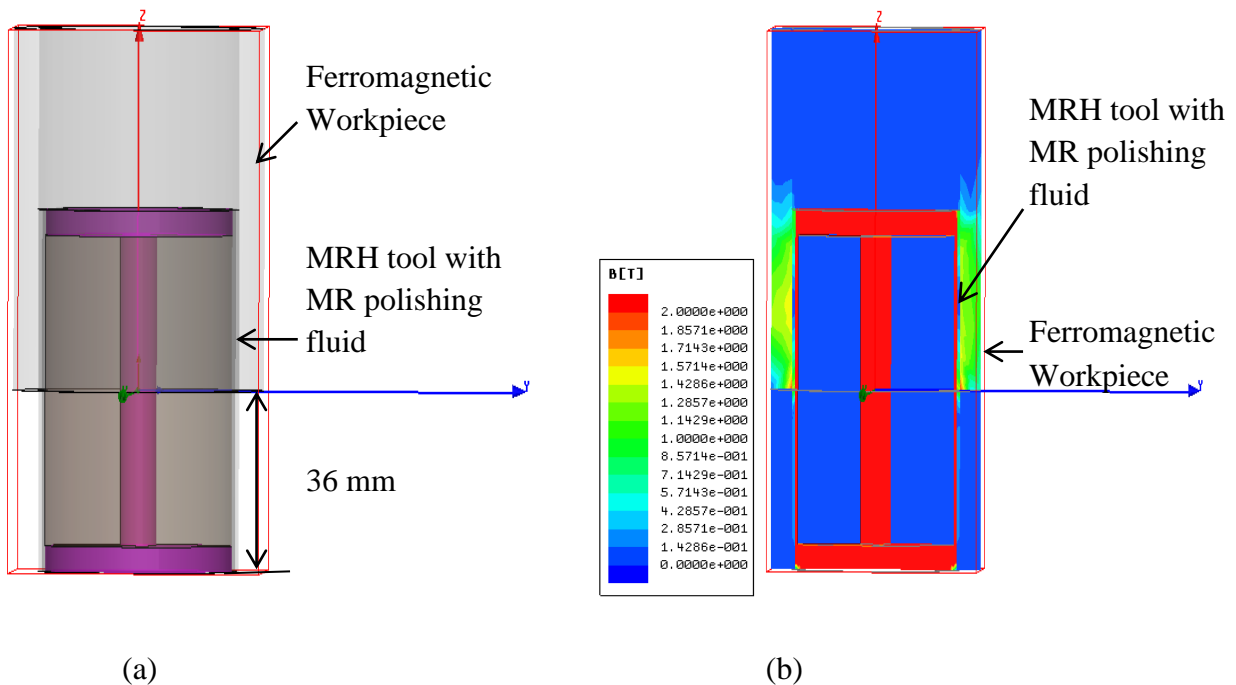


Figure 3.23: MRH tool for ferromagnetic workpiece when base of lower spool is 36 mm below from bottom of the ferromagnetic workpiece (a) Electromagnet model (b) Magnetic flux density distribution

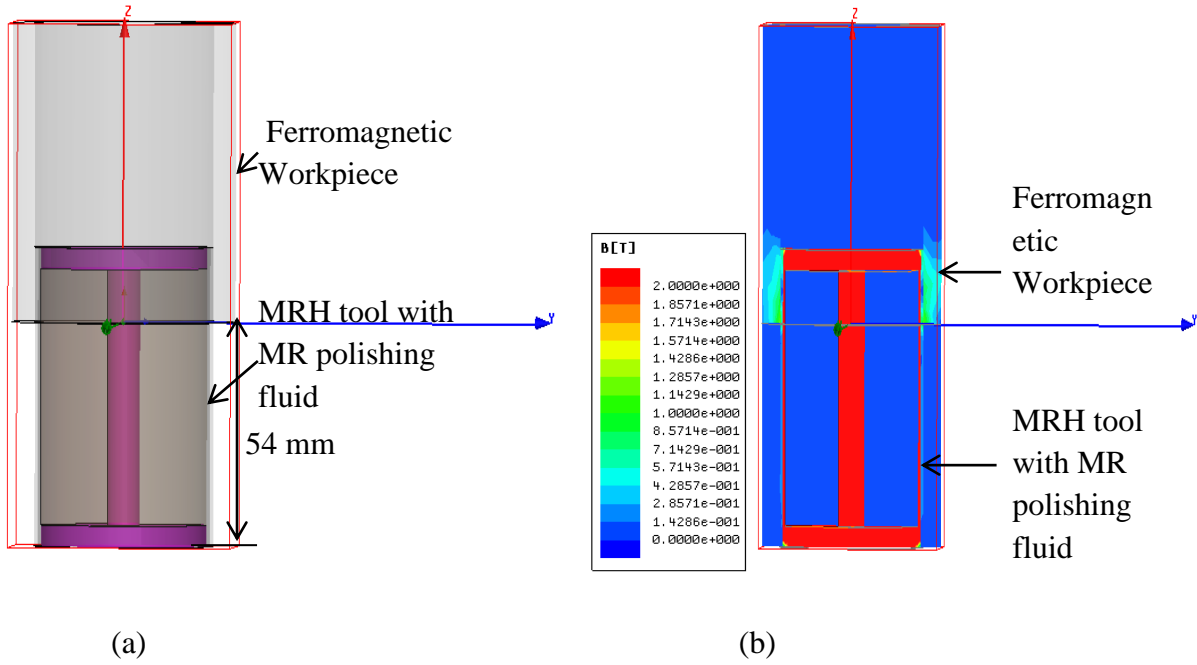


Figure 3.24: MRH tool for ferromagnetic workpiece when base of lower spool is 54 mm below from bottom of the ferromagnetic workpiece (a) Electromagnet model (b) Magnetic flux density distribution

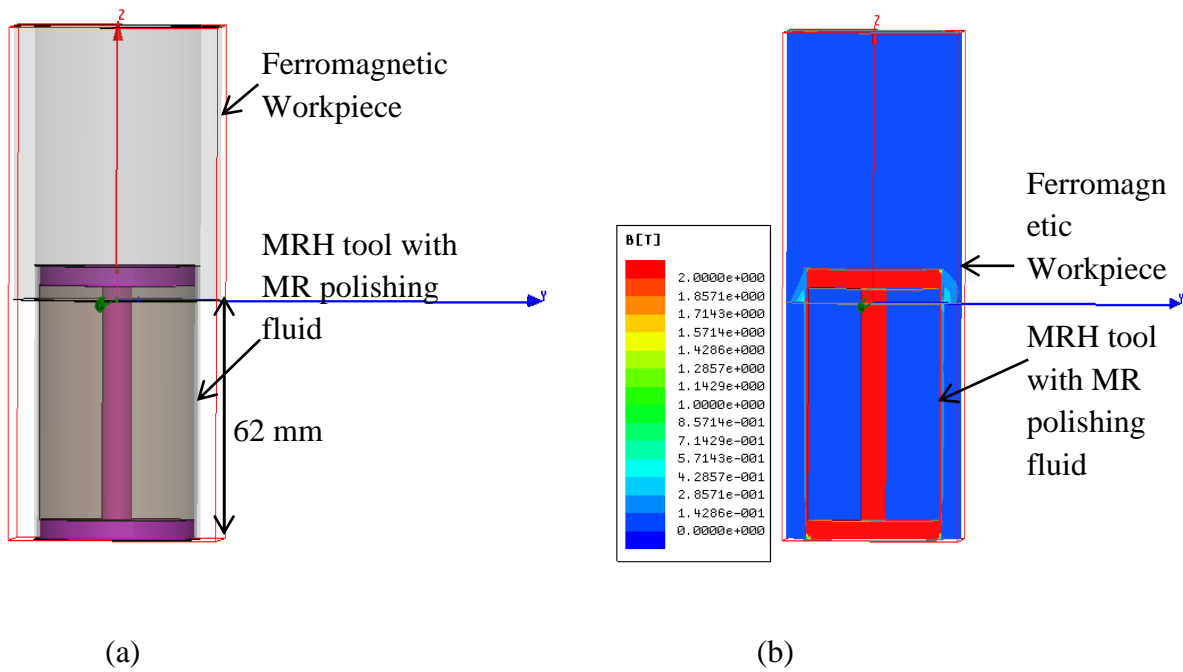


Figure 3.25: MRH tool for ferromagnetic workpiece when base of lower spool is 62 mm below from bottom of the ferromagnetic workpiece (a) Electromagnet model (b) Magnetic flux density distribution

Removal of material and finishing of surface in magnetorheological honing process is mainly due to abrasion which is directly proportional to the time duration for which abrasive particles are in contact with ferromagnetic workpiece surface. From FE simulations of MRH tool performed in Fig. 3.18 to Fig. 3.25, it has been concluded that during the motion of MRH tool inside the ferromagnetic workpiece, magnitude of magnetic flux density is always more at the outer core of MRH tool. Due to higher magnetic flux density at MRH tool, magnetic CI particles move to the high gradient magnetized outer surface of the MRH tool. Under the influence of magnetic field, the magnetic flux density inside the nonmagnetic silicon carbide abrasive particles is very small. That is why most of the abrasive particles get repelled from higher gradient of magnetized outer core surface of MRH tool and moves to the lower gradient of magnetic flux density (inner surface of cylindrical ferromagnetic workpiece) [Nathan Ida]. These abrasives which are on the surface of cylindrical ferromagnetic workpiece are called active abrasive particles and are mainly responsible for removal of material during the movement of MRH tool inside ferromagnetic workpiece. The CIP chain structure tightly grips the active silicon carbide (SiC) abrasive particles towards the inner surface of cylindrical ferromagnetic workpiece surface. When these grabbed active abrasive particles have relative motion with workpiece surface due to the rotation and reciprocation of MRH tool, the peaks of the ferromagnetic workpiece surface get removed out. The higher yield strength of MRP-fluid is at higher gradient magnetized outer surface of MRH tool. The carbonyl iron particle chain will hold silicon carbide abrasive particles strongly and performs the finishing action.

Chapter-4

Mathematical Modeling of Magnetorheological Honing Process

4.1 Mathematical Modeling

After optimizing the tool dimensions in Maxwell ANSOFT V13 software, calculation of forces acting on CIPs and SiCs particles has been calculated mathematically. A schematic diagram of magnetorheological honing (MRH) tool is shown in Fig.4.1. Forces acting on SiCs and CI particles due to magnetic field make them to intent in workpiece surface. Due to the rotatory motion of MRH tool in cylindrical workpiece, a tangential force acts on SiC particles which makes the intended SiC particles to chip off the workpiece surface, material removal and performs finishing action. Mathematical modeling of forces gives a way to analyze the forces required for finishing action and how these forces can be increased or decreased to get the required precise finishing.

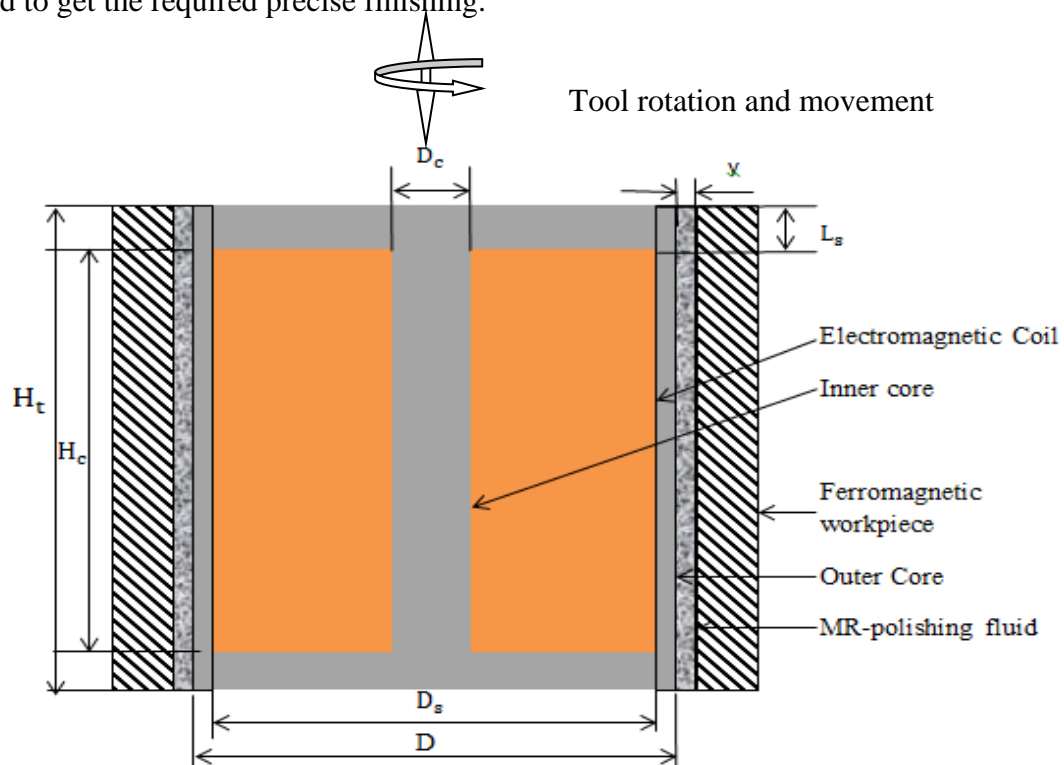


Figure 4.1: Schematic diagram of Magnetorheological Honing tool with workpiece

Tool movement is shown i.e. how it is being rotated and reciprocated. Magnetorheological honing tool consists of core (inner and outer) and electromagnetic coil. In this figure magnetorheological tool is shown with MR polishing fluid flow passage and the workpiece. In Figure 4.1 thickness of MR polishing fluid is shown by y . This thickness y is variable but in mathematical calculations value of y is taken to be 1mm as this value has been optimized in chapter 3. This is the region where MR polishing fluid is allowed to flow through to perform the finishing action on the internal surface of the workpiece.

4.2 Chain Structure and Unit Cell Modeling

MR polishing fluid is present between MRH tool and ferromagnetic workpiece. The study of chain formed in MR polishing fluid by SiC and CIPs on application of magnetic field in MR polishing fluid need to understand for knowing the force applied on workpiece surface for finishing action. It is known that under the influence of external magnetic field, carbonyl iron particles acquire magnetic dipole moment. Whenever forces of dipolar interaction increases so much, the particles align themselves into chains in the direction of field [Furst and Gast, 2000]. Columnar structures are then formed by these chains along the magnetic line of forces at the place where high concentration of carbonyl iron particles is there. For simplifying modeling and simulation of chain structure, it is assumed that CI particles rearrange themselves around the SiC particles in magnetic field direction and repeat in the form of unit cell spanning from workpiece to the outer core [Jha and Jain, 2006]. In real practice due to the existence of non-magnetic abrasives, chains are rarely continuous in MR polishing fluid. Abrasive SiC particles terminate the chain if it comes in between the chain. It can be observed under optical microscope as shown in Fig.4.2.

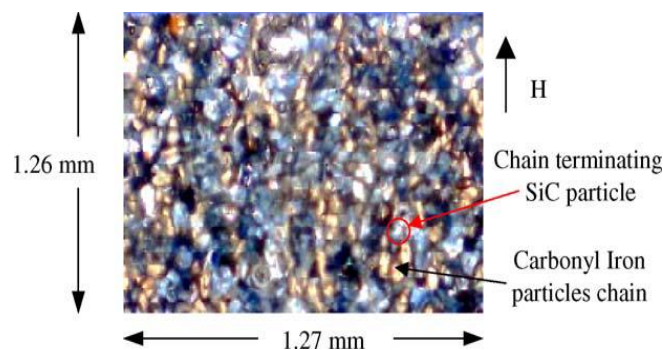


Figure 4.2: Optical micrograph showing termination of CI particles chain due to the existence of non-magnetic abrasives in MR Fluid [Jha and Jain, 2006]

Assumed CI particles and SiC particles arrangement present between workpiece surface and the outer core surface forming the unit cell is shown in Fig.4.3. It has been referred from [Jha and Jain, 2006]. Chain is made by aligning the spherical carbonyl iron particles and SiC particles end-to-end diametrically. A little bit movement of non-magnetic abrasives SiC particles has been assumed on application of magnetic field. SiC particles get stratagem in CIP chain under the influence of magnetic field.

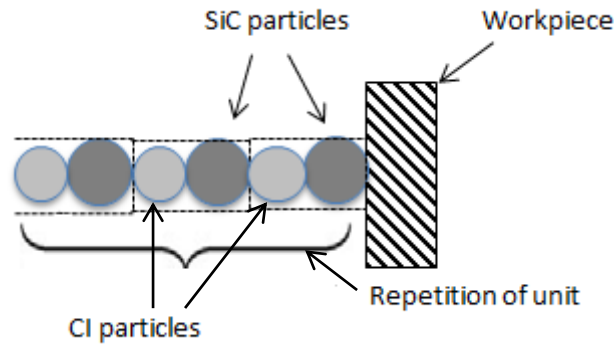


Figure 4.3: Carbonyl iron particles and silicon carbide particle arrangement in MRP fluid with repetition of unit cubic cell on application of magnetic field

4.3 Mathematical Modeling of Magnetorheological Honing Tool

For calculating forces acting on Si and Ci particles, firstly the number of CI and Si particles are calculated present in the finishing region. After that calculation of magnetic flux density present in the finishing region is derived. For simplifying the calculations in mathematical modeling, following assumptions have been made:

- Uniform distribution of carbonyl iron particles (CIPs) and silicon carbide particles (SiCs) has been in MR polishing fluid.
- Average diameter of silicon carbide particles and carbonyl iron particles has been assumed (of spherical shape) of $190\ \mu\text{m}$ and $180\ \mu\text{m}$ respectively. The particles size has been taken 10 times of the actual CS grade size because of the region that software Maxwell ANSOFT V13 could not simulate such a small size of $18\ \mu\text{m}$ or $19\ \mu\text{m}$.
- The other forces like centrifugal and gravitational forces are assumed to be negligible.
- Leakages and losses of magnetic field were not taken into account.

- It is assumed that constant magnetic flux is there throughout the magnetic circuit and is assumed so, so that bottleneck effect of saturation of one region of the magnetic circuit does not occur.
- It is assumed that under the influence of magnetic field a SiC particle indent into the cylindrical workpiece surface due to force acting on CI particle.

The configuration of MR-polishing fluid is shown in Table 4.1

Table 4.1: Configuration of MR polishing fluid

Constituent	% volume concentration
Carbonyl iron particles of CS grade	20
Abrasive silicon carbide particles (SiC) of mesh number 800	20
Base fluid (paraffin oil and AP3 grease)	60

4.3.1 Number of carbonyl iron particles (CIPs) chains present in the working gap

Volume of MR polishing fluid in finishing zone, $V=A \times y$, where A = area of the region where MRP-fluid is there on the outer periphery of the tool with diameter 'D'. y is the thickness of MRP- fluid in between tool and workpiece.

y = thickness of variable finishing gap in mm

D = Outer diameter of tool over which MRP-fluid will flow

H_t =Height of the tool

$$\text{Area, } A = \pi D H_t \text{ mm}^2 \quad (4.1)$$

$$\text{Volume, } V = A y \text{ mm}^3 \quad (4.2)$$

During the optimization of tool in chapter 3, value of outer diameter of the tool has been found to be $D=54$ mm and height of the tool $H_t= 72$ mm. Putting the value of D and H_t in equation number 4.1.

$$\begin{aligned} \text{Area, } A &= \pi \times 54 \times 72 \text{ mm}^2 \\ &= 12214.51224 \text{ mm}^2 \end{aligned} \quad (4.3)$$

Value of y has been optimized to be 1mm. putting the value of $y=1$ mm in equation 4.2.

$$\text{Volume, } V= 12214.51224 \text{ mm}^3 \quad (4.4)$$

Numbers of (CIPs) present in volume V of MRP-fluid [Singh et al., 2012].

$$N_{\text{CIP}} = \frac{\% \text{ volume fraction of CIP in MRP fluid} \times V}{\text{Volume of single CIP particle}} \quad (4.5)$$

$$\text{Volume of single CIP particle} = \frac{4}{3} \pi \left(\frac{d_c}{2} \right)^3 = 3.0536 \times 10^{-3} \text{ mm}^3$$

$$d_c = \text{diameter of CI particle} = 180 \mu\text{m} = 180 \times 10^{-3} \text{ mm}$$

$$\text{Therefore, } N_{\text{CIP}} = 800000 \quad (4.6)$$

$$\text{Number of CI particles in one chain} = \frac{y}{d_c} = 6 y \text{ [Singh et al., 2012].} \quad (4.7)$$

Total number of CI particle chains formed with 20% volume fraction of CI particles in volume V of MRP-fluid is given by [Singh et al., 2012].

$$N_{(\text{CIP})\text{chains}} = \frac{N_{\text{CIP}}}{\text{Number of CIPs in one chain}} = \frac{800000}{6y} \quad (4.8)$$

Putting the value of $y = 1$ mm in above equation

$$N_{(\text{CIP})\text{chains}} = 133333 \quad (4.9)$$

4.3.2 Number of active abrasives per chain of CIPs present on the surface of workpiece

During the finishing operation numbers of active SiC abrasives present on the surface of workpiece responsible for removal of material is given by [Singh et al., 2012].

$$N_{AAB} = \frac{\% \text{ volume fraction of SiC in MRP fluid} \times A \times \text{diameter of SiC}}{\text{Volume of single SiC particle}} \quad (4.10)$$

$$\text{Volume of single SiC particle} = \frac{4}{3} \pi \left(\frac{d_s}{2} \right)^3 = 3.589 \times 10^{-3} \text{ mm}^3$$

$$d_s = \text{diameter of single SiC particle} = 190 \mu\text{m} = 190 \times 10^{-3} \text{ mm}$$

$$\text{Therefore } N_{AAB} = 129306 \quad (4.11)$$

Therefore, number of active SiC abrasives per chain of CIPs on the workpiece surface is given by [Singh et al., 2012].

$$= \frac{N_{AAB}}{N_{(CIP)chains}} \quad (4.12)$$

Putting the values of N_{AAB} and $N_{(CIP)chains}$ from equations 4.11 and 4.9, number of active abrasive particles (SiC) per chain of CIPs will be

$$= \frac{129306}{133333} = 0.9698 \quad (4.13)$$

It can be approximately taken as 1. It means that for one active abrasive particle, there will be one chain of CIPs over it.

4.3.3 Calculation of magnetic flux density

After designing and optimizing the tool in Maxwell ANSOFT V13, a simplified geometric representation and magnetic circuit of magnetorheological honing tool is drawn as shown in Fig. 4.4. In this figure, flow of magnetic field is shown in the form of magnetic circuit and is shown how magnetic flux is flowed through different surface areas of different materials. Magnetic field lines are supposed to flow through two sides of the core in two different magnetic circuits which are symmetrical about central axis. For calculating magnetic flux, one side of magnetic circuit is considered.

Magnetic circuit of the magnetorheological honing tool structure is shown in Fig.4.4. The magnetic circuit of MRH tool can be analyzed using the magnetic Kirchoff's law as follows:

$$\sum H_k l_k = NI \quad (4.14)$$

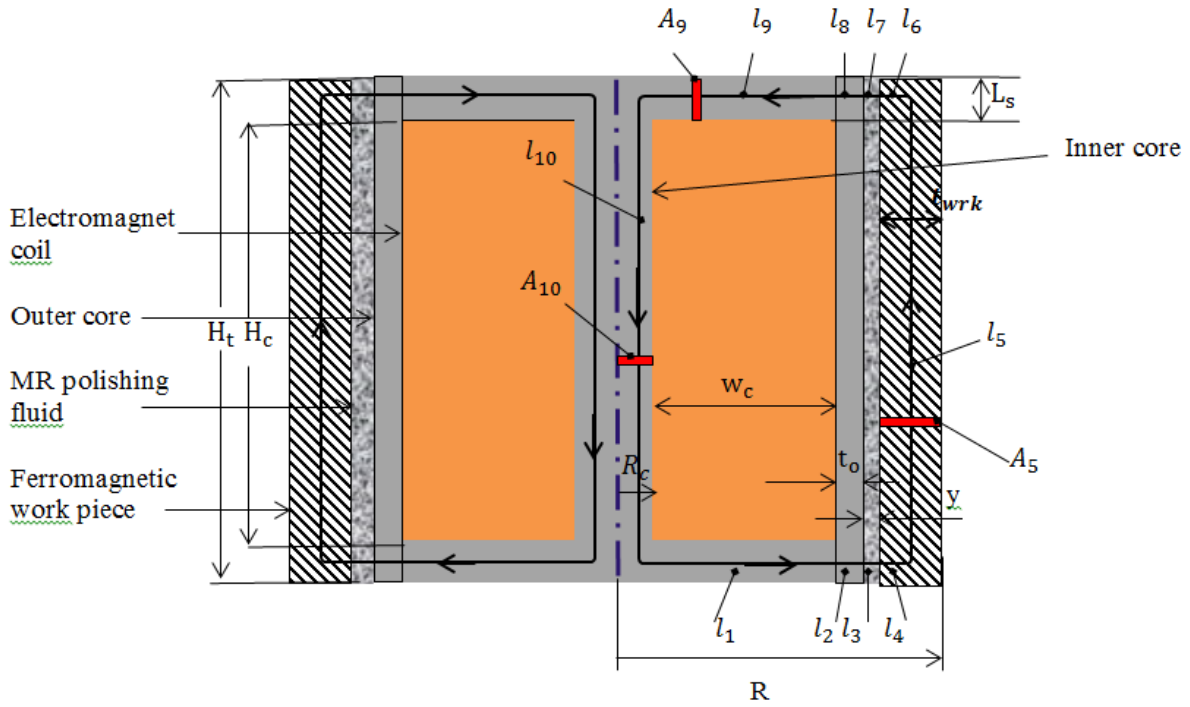


Figure 4.4: The simplified geometric presentation and magnetic circuit of the Magnetorheological Honing Tool with Ferromagnetic Workpiece

- Here
- R = radius of complete setup
 - H_c = height of central inner part of core
 - H_t = total height of the tool
 - R_c = radius of central part of inner core
 - L_s = thickness of the spool
 - D_c = diameter of central part of inner core structure
 - w_c = width of coil

where H_k is the magnetic field intensity in the k^{th} link of the circuit and l_k is the overall effective length of that link. N is the number of turns in the coil of magnetorheological honing tool and I is electromagnet current given to coil. The magnetic flux is conserved in the circuit as follows

$$\Phi = B_k A_k \quad (4.15)$$

where Φ is the magnetic flux of the circuit, A_k and B_k are the cross-sectional area and magnetic flux density of the k^{th} link, respectively. In this study, magnetic circuit of MR honing tool is divided into 10 links as shown in Figure 4.4. In this case, Equations (4.14) and (4.15) can be rewritten by

$$H_1l_1 + H_2l_2 + H_3l_3 + H_4l_4 + H_5l_5 + H_6l_6 + H_7l_7 + H_8l_8 + H_9l_9 + H_{10}l_{10} = NI \quad (4.16)$$

$$\Phi = B_1A_1 = B_2A_2 = B_3A_3 = B_4A_4 = B_5A_5 = B_6A_6 = B_7A_7 = B_8A_8 = B_9A_9 = B_{10}A_{10} \quad (4.17)$$

In the above, the effective length and cross-sectional area of magnetic links are given as following:

$$l_1 = l_9 = \frac{R_c}{2} + w_c; \quad l_2 = l_8 = t_o; \quad l_3 = l_7 = y; \quad l_4 = l_6 = \frac{t_{wrk}}{2}; \quad l_5 = l_{10} = H_t - L_s$$

$$A_1 = A_9 = 2lR_1L_s; \quad A_2 = A_8 = 2lR_{d1}L_s; \quad A_3 = A_7 = 2lR_{d2}L_s \quad (4.18)$$

$$A_4 = A_6 = 2lR_3L_s; \quad A_5 = \pi(R^2 - R_4^2); \quad A_{10} = \pi\left(\frac{R_c}{2}\right)^2$$

Where,

$$R_1 = R_c + \frac{w_c}{2}; \quad R_{d1} = R_c + w_c + \frac{t_o}{2}; \quad R_{d2} = R_c + w_c + t_o + \frac{y}{2} \quad (4.19)$$

$$R_3 = R - \frac{t_{wrk}}{2}; \quad R_4 = R - \frac{3t_{wrk}}{4}$$

Condition where low magnetic field is there, the magnetic flux density, B_k , increases proportionally with magnetic intensity H_k as follows [Nguyen and Choi, 2012]

$$B_k = \mu_0 \mu_k H_k \quad (4.20)$$

where μ_0 is the magnetic permeability of free space ($\mu_0 = 4\pi 10^{-7} \text{Tm/A}$) and μ_k is the relative permeability of the k^{th} link material. From Equations (4.16) and (4.17) and the B-H curves of the MR polishing fluid and the MR honing tool structure material, the magnetic circuit can be solved. Considering the equation no. 4.18, the magnetic flux density and the field intensity of the k^{th} link of magnetic circuit can be calculated as follows [Nguyen and Choi, 2012]

$$B_k = \frac{\mu_0 NI}{l_k + \sum_{i=1, i \neq k}^{10} \frac{l_i A_k}{\mu_i A_i}} \quad (4.21)$$

$$H_k = \frac{NI}{l_k + \sum_{i=1, i \neq k}^{10} \frac{\mu_k A_k l_i}{\mu_i A_i}} \quad (4.22)$$

Relative permeability of the MR honing tool structural material has been assumed to be similar ($\mu_1 = \mu_2 = \mu_4 = \mu_5 = \mu_6 = \mu_8 = \mu_9 = \mu_{10} = \mu = 600$) and putting into equation 4.21, the magnetic

flux density of outer tool, region where MR polishing fluid is present and the ferromagnetic workpiece link of magnetic circuit respectively can be calculated as follows

$$B_{\text{outer tool}} = B_2 = \frac{\mu_0 NI}{\frac{2t_0}{\mu} + \frac{2yA_2}{\mu_{\text{MRA}_3}} + \frac{2l_1A_2}{\mu A_1} + \frac{2l_4A_2}{\mu A_4} + \frac{l_5A_2}{\mu A_5} + \frac{l_{10}A_2}{\mu A_{10}}} \quad (4.23)$$

$$B_{\text{MR}} = B_3 = \frac{\mu_0 NI}{\frac{2y}{\mu_{\text{mr}}} + \frac{2l_1A_3}{\mu A_1} + \frac{2l_2A_3}{\mu A_2} + \frac{2l_4A_3}{\mu A_4} + \frac{l_5A_3}{\mu A_5} + \frac{l_{10}A_3}{\mu A_{10}}} \quad (4.24)$$

$$B_{\text{wrk}} = B_4 = \frac{\mu_0 NI}{\frac{2l_4}{\mu} + \frac{2l_1A_4}{\mu A_1} + \frac{2l_2A_4}{\mu A_2} + \frac{2yA_4}{\mu_{\text{mr}A_3}} + \frac{l_5A_4}{\mu A_5} + \frac{l_{10}A_4}{\mu A_{10}}} \quad (4.25)$$

After optimizing the tool in chapter-3, MRH tool with ferromagnetic workpiece is modeled in MAXWELL ANSOFT V13 software with the dimensions as shown in Fig 4.5. All dimensions shown are in mm.

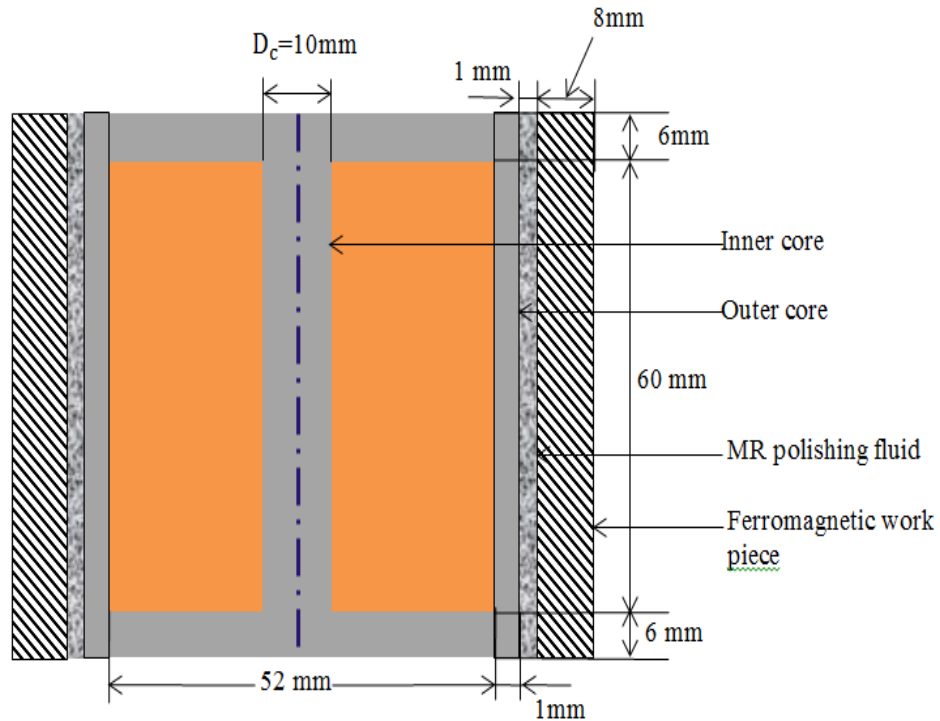


Figure 4.5: Geometric presentation of Magnetorheological Honing Tool with Ferromagnetic Workpiece

Taking all values from Fig. 4.5 and putting in equations 4.18

$$\text{Here } R_c = \frac{D_c}{2} = 5\text{mm}$$

$$l_1 = l_9 = \frac{R_c}{2} + w_c = 23.5\text{m}$$

$$l_2 = l_8 = t_o = 1\text{mm}$$

$$l_3 = l_7 = y = 1\text{mm}$$

$$l_4 = l_6 = \frac{t_{\text{wrk}}}{2} = 4\text{mm}$$

$$A_1 = A_9 = 2\pi R_1 L_s = 584.33\text{mm}^2$$

$$A_2 = A_8 = 2\pi R_{d1} L_s = 999.02 \text{ mm}^2$$

$$A_3 = A_7 = 2\pi R_{d2} L_s = 1036.725576 \text{ mm}^2$$

$$A_4 = A_6 = 2\pi R_3 L_s = 1130.97 \text{ mm}^2$$

$$A_5 = \pi(R^2 - R_4^2) = 854.51 \text{ mm}^2$$

$$A_{10} = \pi\left(\frac{R_c}{2}\right)^2 = 19.63 \text{ mm}^2$$

where,

$$R_1 = R_c + \frac{w_c}{2} = 15.5 \text{ mm}$$

$$R_{d1} = R_c + w_c + \frac{t_o}{2} = 26.5 \text{ mm}$$

$$R_{d2} = R_c + w_c + t_o + \frac{y}{2} = 27.5 \text{ mm}$$

$$R_3 = R - \frac{3t_{\text{wrk}}}{4} = 30 \text{ mm}$$

$$R_4 = R - \frac{t_{\text{wrk}}}{2} = 32 \text{ mm}$$

N is the number of turns in the coil which is equal to $H_c \times w_c = 21 \times 60 = 1260$ and I is the current given to the each coil which is equal to 4 A as defined earlier. Putting all these values in equation (4.23), (4.24), (4.25) we get the value of magnetic flux density at outer core, MR polishing fluid region and ferromagnetic workpiece respectively as follows

$$B_{\text{outer core}} = B_2 = 1.4 \text{ Tesla}$$

$$B_{\text{MR}} = B_3 = 0.97 \text{ Tesla}$$

$$B_{\text{wrk}} = B_4 = 0.80 \text{ Tesla}$$

Magnetic flux density in MR polishing fluid region is calculated by equation (4.26) as shown below:

$$B_{MR} = B_3 = \frac{\mu_0 NI}{\frac{2y}{\mu_{mr}} + \frac{2l_1 A_3}{\mu A_1} + \frac{2l_2 A_3}{\mu A_2} + \frac{2l_4 A_3}{\mu A_4} + \frac{l_5 A_3}{\mu A_5} + \frac{l_{10} A_3}{\mu A_{10}}} \quad (4.26)$$

A function of magnetic flux density variation (in term of y) in MR polishing region is made by putting up the values of $l_1, l_2, l_3, l_4, l_5, l_6, l_7, l_8, l_9$ and l_{10} , and $A_1, A_2, A_3, A_4, A_5, A_6, A_7, A_8, A_9$ and A_{10} taken above in equation 4.26 as given below.

$$B_{MR} (y) = \frac{\mu_0 NI \times 10^3}{(6.09 + \frac{2y}{\mu_{mr}})} \quad (4.27)$$

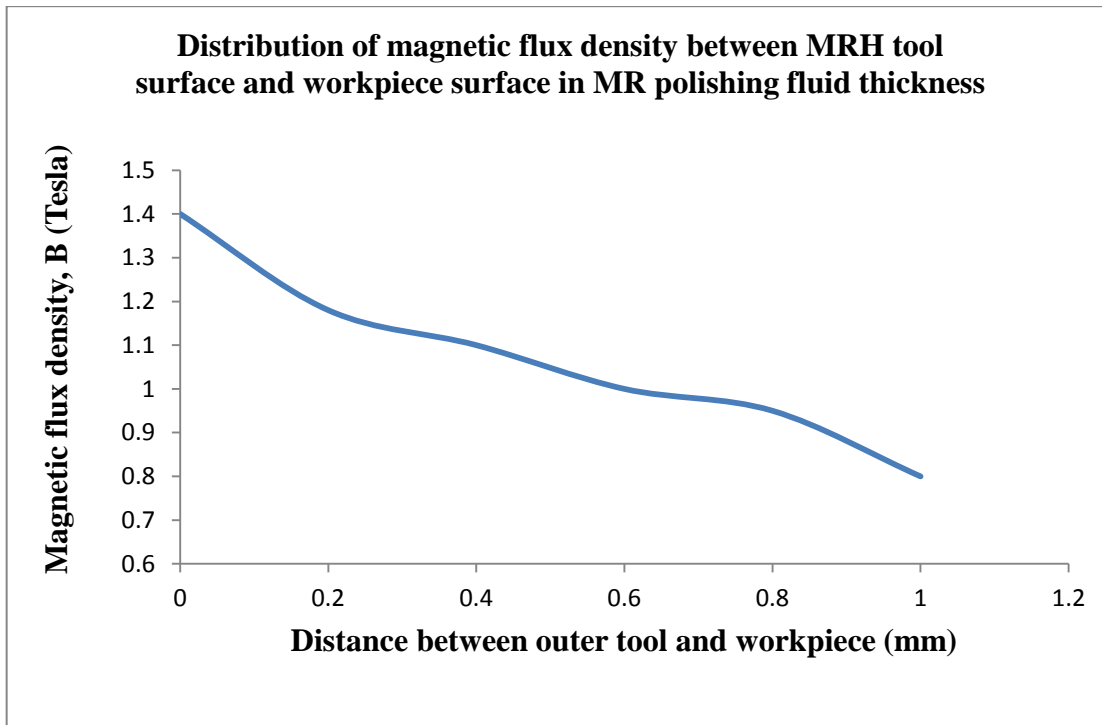


Figure 4.6: Distribution of magnetic flux density between MRH tool surface and workpiece surface in MR polishing fluid (Eq. 4.27)

Theoretical calculated value of magnetic flux density on workpiece, MR polishing fluid region and outer core clearly shows that there is maximum magnetic flux on the outer surface of MRH tool as compared to the workpiece inner surface as shown in Fig.4.6. It shows that MR polishing fluid sticks up to the outer surface of MRH tool and non-ferromagnetic particles i.e. silicon carbide particle comes on inner surface of workpiece and performs the better finishing action.

Differentiating $B_{MR}(y)$ with respect to y

$$\frac{dB_{MR}(y)}{dy} = -\frac{2(\mu_0 N_c I) \times 10^3}{\mu_{mr} \left(6.09 + \frac{2y}{\mu_{mr}}\right)^2} \quad (4.28)$$

4.3.4 Calculation of Force acting on a Carbonyl Iron Particle due to Magnetic Field

Force acting on carbonyl iron particle of mass 'm' present in MR polishing fluid can be calculated by Eq. 4.29 [Stradling, 1993]

$$F_{CIP} = m \mu_0 \chi_m H \nabla H \quad (4.29)$$

Where μ_0 is magnetic permeability of free space and χ_m is magnetic susceptibility of carbonyl iron particles (CIPs), m mass of CIP and H is magnetic field strength. For practical purposes, it is advantageous to replace field strength with magnetic induction using relation $B = \mu_0 H$ [Jha and Jain, 2006] so that Eq. (4.29) becomes

$$F_{CIP} = \frac{m \chi_m}{\mu_0} B \nabla B \quad (4.30)$$

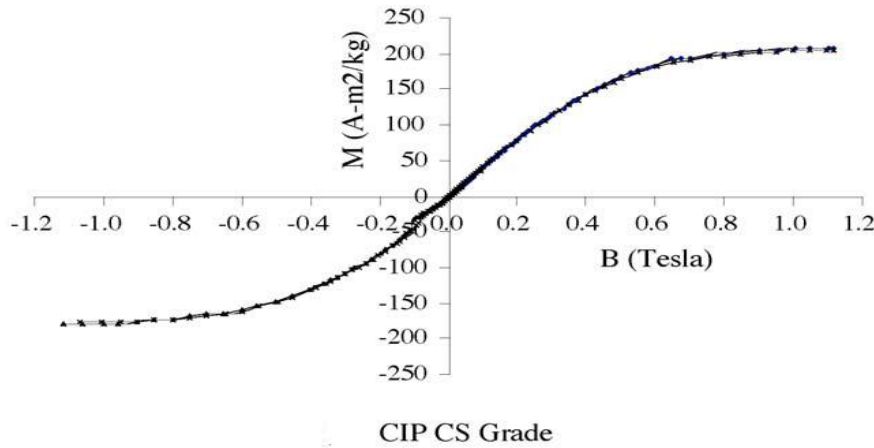


Figure 4.7: M-B curve for CIP of CS Grade [Jha and Jain, 2006]

The variation of B in x direction is negligible, hence after neglecting it Eq. (4.30)

$$F_{CIP}(y) = \frac{m \chi_m}{\mu_0} B_{MR}(y) \frac{dB_{MR}(y)}{dy} \quad (4.31)$$

$$\text{Mass of CI particle, } m = \frac{4}{3} \pi \left(\frac{d_c}{2}\right)^3 \times \rho$$

Here ρ is density of iron which is equal to 7870 kg/m^3 [Jha and Jain, 2006]

Mass of iron particle = 2.40×10^{-8} kg

Using the relation $\chi_m = \frac{\mu_0 M}{B_{MR}(y)}$ [Jha and Jain, 2006], taking the value of M from M-B curve as given in Fig. 4.7 and put in equation 4.31

Calculating the value of $\frac{dB_{MR}(y)}{dx}$ at $y = 0.72$ mm i.e. just after the SiC particle which is adjacent to the inner wall of the workpiece and putting all the values in equation 4.31, force on small ferromagnetic CIP particle can be calculated present in MRP-fluid in y-direction which is equal to

$$F_{CIP} = 2.98 \times 10^{-7} \text{ Newton}$$

This calculated force acting on CI particle will exert force on SiC particle. Hence force acting on SiC particle equals to calculated value of force acting on CI particle. This force on SiC particle exert force on workpiece surface and is called indentation force, F_i .

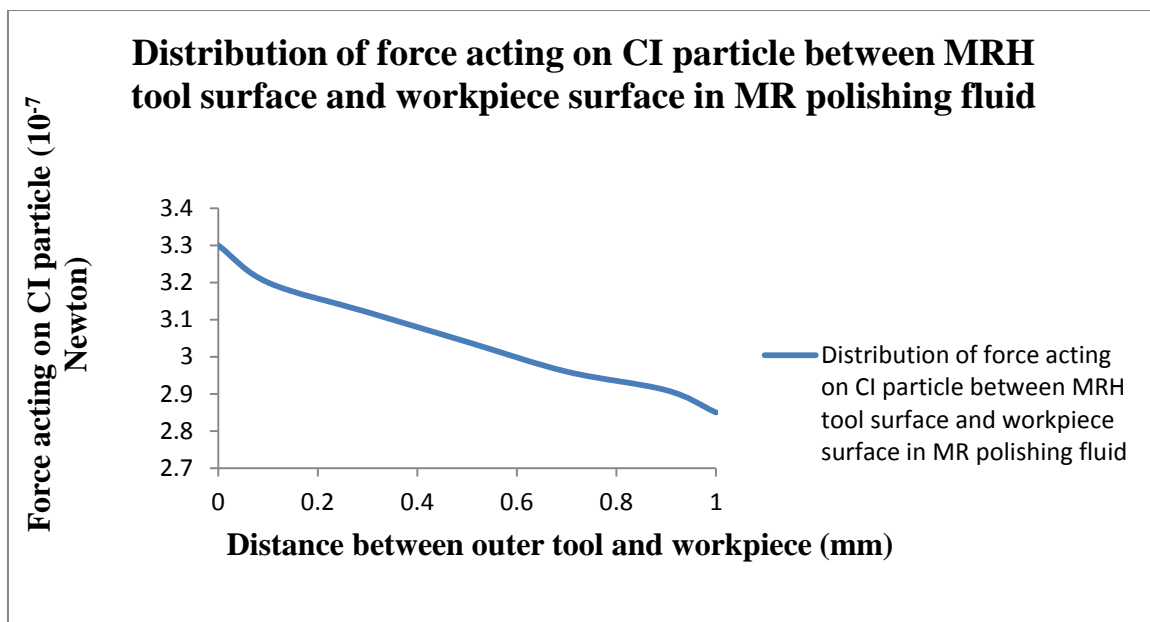


Figure 4.8: Distribution of force acting on CI particle between MRH tool surface and ferromagnetic workpiece surface in MR polishing fluid (Eq. 4.31)

Distribution of force acting on CI particle between MRH tool surface and ferromagnetic workpiece surface in MR polishing fluid is shown in Fig. 4.8. Value of force acting on CI particle goes on decreasing as moving from outer surface of MRH tool to the inner surface of ferromagnetic workpiece because magnetic flux density decreases from outer tool surface to ferromagnetic workpiece surface.

4.4 Surface roughness modeling

Inner surface of the ferromagnetic workpiece is finished by active SiC particles. Under the action of magnetic force acting on CIPs, abrasive SiC particles indent on the surface of workpiece. The magnetically induced force acting on CIPs is transferred to the SiC particles which get in between the CIPs chain. Active SiC particles get indented in the workpiece surface as shown in Fig.4.9 (a). When tool rotates under the magnetic field, MR polishing fluid sticks to the tool also rotates. Due to the hydraulic pressure of MR polishing fluid, penetrated abrasive particles are forced to translate and the removal of workpiece takes place. Removal of material occurs only when tangential force applied by fluid (F_{shear}) is greater than reaction force (R_{shear}).

$$F_{\text{shear}} = (A'' - A')\tau_y \quad (4.32)$$

$$R_{\text{shear}} = A' \sigma_y \quad (4.33)$$

Where A'' is the abrasive grain projected area (total), A' is indented part of abrasive in workpiece surface projected area, σ_y yield stress of workpiece in shear and τ_y is MR polishing fluid shear stress.

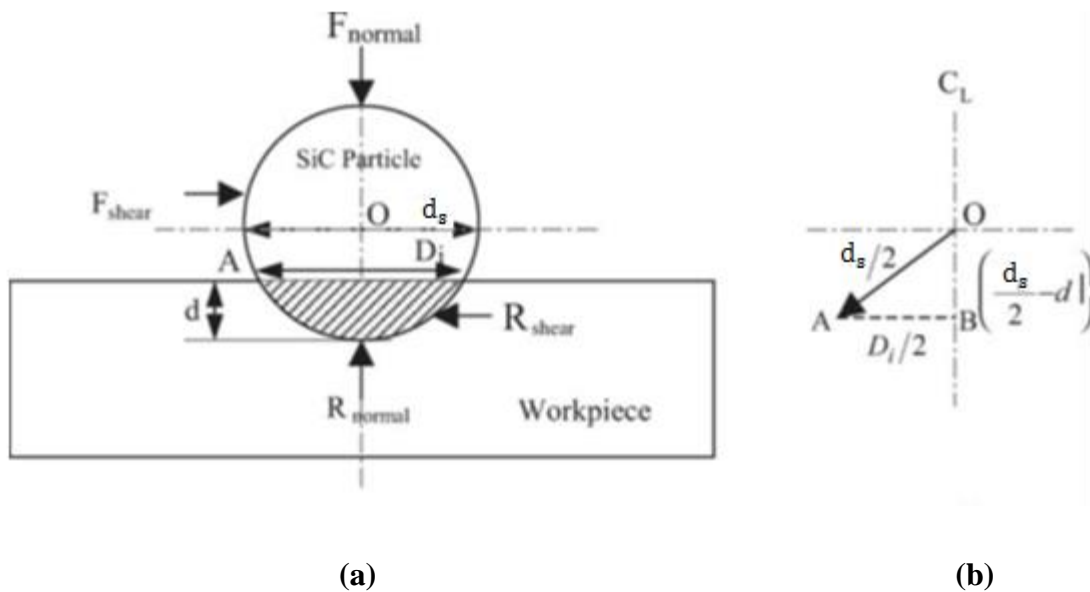


Figure 4.9: (a) Forces acting on abrasives in magnetorheological honing process (b) Calculation of D_i [Jha and Jain, 2006]

Abrasives can remove the surface of workpiece either by shearing or ploughing [Brecker et al, 1969]. The depth of indentation of active SiC particle (d) can be calculated from equation (4.34) as given below [Jha and Jain, 2006]

$$d = \frac{d_s}{2} - \frac{1}{2} \sqrt{d_s^2 - D_i^2} \quad (4.34)$$

where d_s is the abrasive diameter in mm and D_i is the indentation diameter in mm. Indentation diameter D_i can be obtained by equation (4.35) as shown below [Jha and Jain, 2006]

$$D_i = \sqrt{d_s^2 - \left(d_s - \frac{2 \times 10^{-6} F_i}{9.81 H_{BHN} / d_s}\right)^2} \quad (4.35)$$

Where F_i is indentation force on abrasive in newton and H_{BHN} is the workpiece Brinell hardness number in kgf/mm^2 .

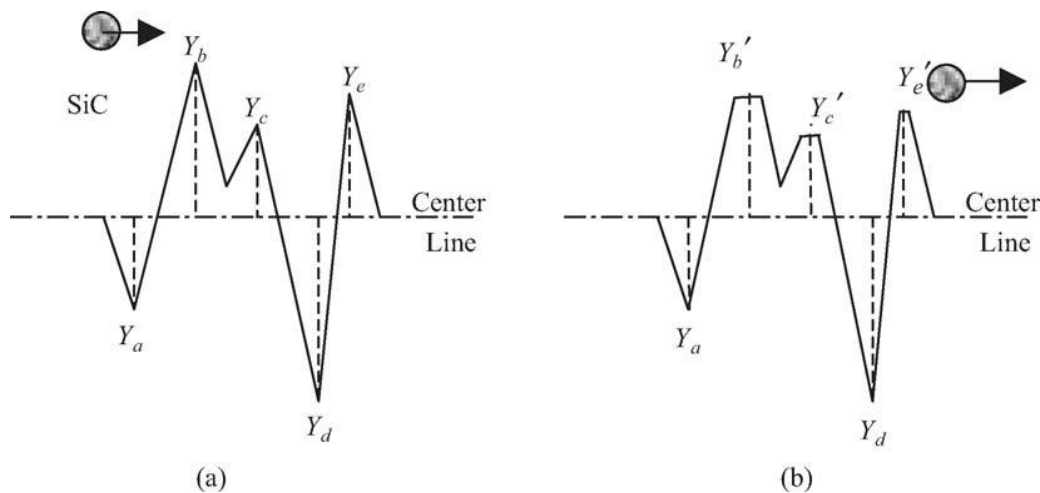


Figure 4.10: (a) Abrasives coming to initial peaks/valleys of height/depth and (b) new peak heights after one indentation depth (d) [Jha and Jain, 2006]

It is assumed that each SiC particle pass on the peaks penetrated equal to d . The new formed peak height Y_i after 1 stroke with N_g active grains/stroke is given by

$$Y'_i = Y_i - N_g d \quad (4.36)$$

If the point is not a peak point in the data file (for example Y_a and Y_d in Fig.4.10), then it is transferred to next profile as it is. Before and after each stroke, the center-line-average (CLA) surface roughness value (R_a) from profile data points was calculated using Eq. (4.37)

$$R_a = \frac{\sum_{i=1, \dots, N'} |Y_i|}{N'} \quad (4.37)$$

where N' is number of data points and Y_i is roughness profile height at the data points

4.5 Results and Discussions

An electromagnet model of MRH tool with ferromagnetic workpiece is modeled in Maxwell ANSOFT V13 with dimensions as obtained from optimization of MRH tool with ferromagnetic workpiece in chapter-3. Columnar structure of silicon carbide (SiC) and carbonyl iron (CI) particles is modeled in MR polishing fluid region as shown in Fig. 4.11. Chain is formed such that SiC particle just touches the workpiece surface. After the SiC particle CI particle is placed and this (SiC and CI particle) forms the unit cell. Unit cell is repeated end to end from ferromagnetic workpiece surface to outer core.

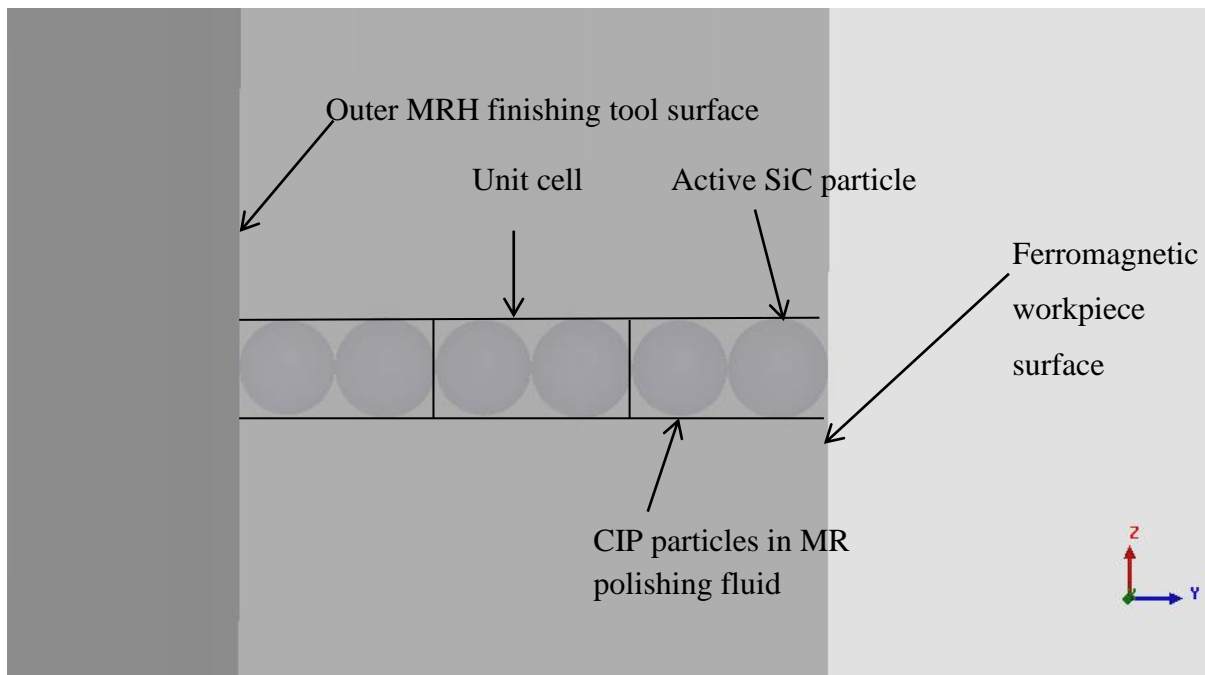


Figure 4.11: Electromagnet model of MRH tool having SiC and CIP particles in columnar structure.

Material assigned to silicon carbide particles have been taken from MAXWELL ANSOFT V13 library as alumina with relative permeability 1 and carbonyl iron particles as iron with relative permeability 4000. Silicon carbide particles are modeled with average diameter of 190 μm and carbonyl iron particles with average diameter of 180 μm . Parameters assigned to the electromagnet model of MRH tool with ferromagnetic workpiece are given in Table 3.1.

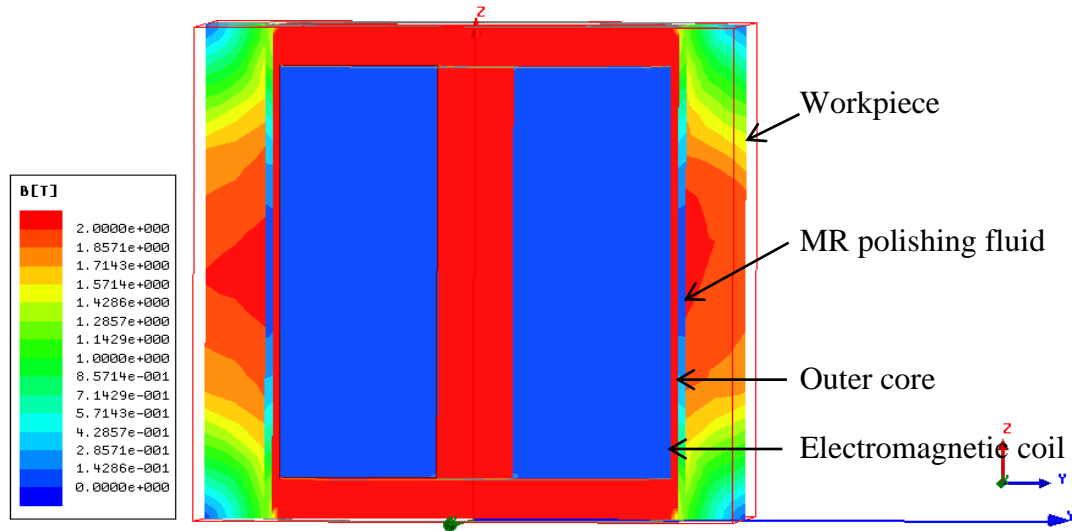


Figure 4.12: Magnetic flux density distribution of MRH tool for ferromagnetic workpiece

MRH tool with ferromagnetic workpiece is magneto statically simulated and force on SiC and CI particle is then observed. These values of forces obtained from FE analysis is then compared with theoretical calculated values of forces on CI particle by mathematical modeling and is shown in Fig. 4.13.

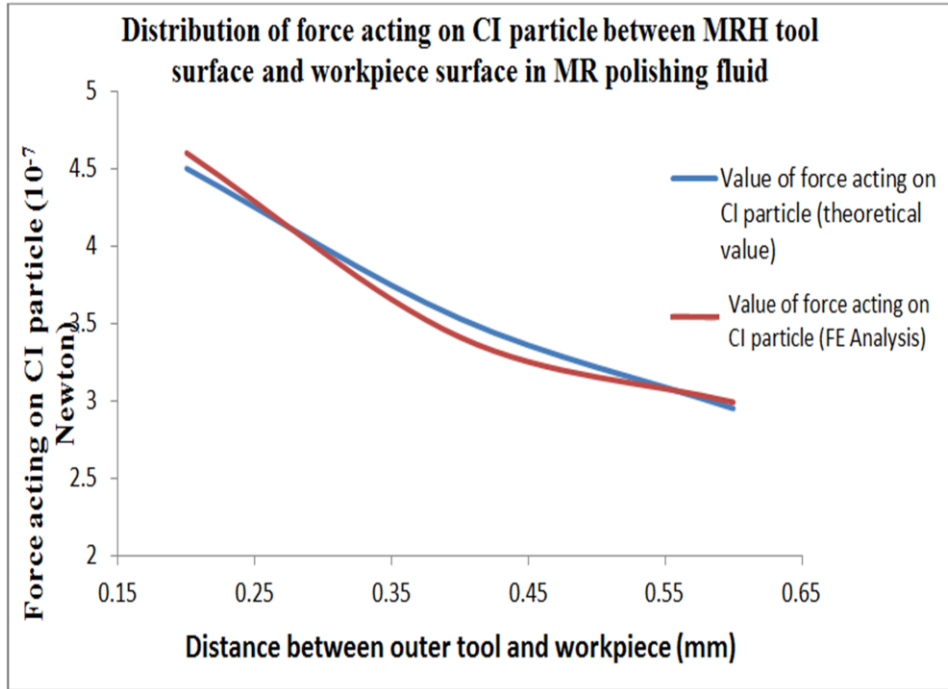


Figure 4.13: Distribution of magnetic flux density of MRH tool for ferromagnetic workpiece between outer finishing tool surface and ferromagnetic workpiece surface

It is clear from Fig. 4.13 that theoretical calculated value of magnetostatically induced forces on CI particles present in columnar structure between MRH tool surface and ferromagnetic workpiece surface is very close to value of forces obtained from FE analysis of MRH tool with ferromagnetic workpiece.

Chapter-5

Conclusions and Future Scope

5.1 Conclusions

The present work is done to optimize and mathematically model a novel magnetorheological honing process. From finite element analysis (using Maxwell ANSOFT V13 software) and mathematical modeling of magnetorheological honing process, following points have been concluded as given below:

- Tool dimensions have been finalized for the fabrication as per the optimized value of dimensions obtained from finite element analysis for distribution of maximum flux density in magnetorheological honing tool with workpiece surfaces.
- Analyzed the distributions of magnetic flux density gradient in the magnetorheological polishing fluid layer between the outer tool surface and inner surface of workpiece, it has been found that outer tool surface has maximum flux density gradient as compared to the inner workpiece surface (having low flux density gradient).
- From the distributions of magnetic flux density gradient between outer tool surface and inner workpiece surface, it has been concluded that magnetorheological polishing fluid always retain on outer finishing tool surface as it has maximum flux density. This is very important factor to perform the finishing operation on the workpiece surfaces as CIPs chains strongly grip the active abrasives on workpiece surfaces.
- From the mathematical modeling of magnetorheological honing process, it has been found that magnitude of magnetic flux density goes on decreasing from outer tool finishing surface to the inner surface of workpiece confirming that magnetorheological polishing fluid always retain on outer tool surface with irrespective of types of workpiece surfaces.

5.2 Future Scope

The present work is the preliminary analysis of the newly developed magnetorheological honing process. Therefore, many in depth analysis yet to be done such as :

- Experimental validation with the theoretical mathematical model for magnetorheological honing process can be compared in future.
- Complete realistic mathematical model of surface roughness can be done and compare experimentally for the developed magnetorheological honing process.
- Forces acting on workpiece surfaces during finishing operation needs to be analyzed experimentally in details and their effects on change in surface roughness value.

References

- Brecker, J.N.; Brown, R.; Matsuo, T.; Saito, K. (1969) Fourth Annual Report of Abrasive Grain Association on Investigation of Abrasive Grain Characteristics, Carnegie Institute of Technology, USA, November
- Cheng, H.; Yeung, Y.; Tong, H. (2008) Viscosity behavior of magnetic suspensions in fluid assisted finishing, *Progress in Natural Science*, 18: 91-96.
- Das, M.; Jain, V.K.; Ghoshdastidar, P.S. (2008) Fluid flow analysis of magnetorheological abrasive flow finishing process. *International Journal of Machine Tools and Manufacture*, 48: 415-426.
- Furst, E.M.; Gast, A.P. (2000), Micromechanics of magnetorheological suspensions, *Phys. Rev. E*61/6: 6732–6739.
- Gheisari, R.; Ghasemi, A.A.; Jafarkarimi, M.; Mohtaram, S. (2014) Experimental studies on the ultraprecision finishing of cylindrical surfaces using magnetorheological finishing process. *Production & Manufacturing Research*, 2: 550-557.
- Jain, R.K.; Jain V.K.; Dixit P.M. (1999) Modeling of material removal and surface roughness in abrasive flow machining process, *International Journal of Machine Tools and Manufacture*, 39: 1903-1923.
- Jain, V.K. (2009) Magnetic field assisted abrasive based micro-/nano-finishing. *Journal of Materials Processing Technology*, 209: 6022-6038.
- Jha S.; Jain, V.K. (2006), Modeling and simulation of surface roughness in magnetorheological abrasive flow finishing (MRAFF) process, *Wear*, 261: 856-866.
- Judal, K.B.; Yadava, V.; Pathak, D. (2013), Experimental investigation of vibration assisted cylindrical magnet abrasive finishing of Aluminium workpiece. *Materials and Manufacturing Processes*, 28: 1196-1202.
- Kang, J.; George, A.; Yamaguchi, H. (2012) High-speed internal finishing of capillary tubes by magnetic abrasive finishing. *Procedia CIRP*, 1: 414-418.
- Kordonski, W. I.; Shorey, A. B.; Tricard, M. (2004) Magnetorheological (MR) Jet Finishing Technology, *ASME International Mechanical Engineering Congress*, 78: 13-19.

- Mori, Y.; Yamauchi, K.; Endo, K. (1987) Elastic Emission machining. *Precision Engineering* 9(3):123-128.
- Nathan Ida, Engineering Electromagnetics, Springer, New York, 2004. (Chapter 9).
- Nguyen, Q.H.; Choi, S.B., (2009) Analytically optimal design of MR valve and damper, *Smart material and structures*, 54:402-751.
- Nowicki, B. (1993) The new method of freeform surface honing, *CIRP Annals Manufacturing Technology*, 42: 425–428.
- Pattanaik , L.N.; Agarwal, H. (2014) Development of magnetorheological finishing (MRF) process for freeform surfaces, *International Journal of Advanced Mechanical Engineering*, 4: 611-618.
- Sadiq, A.; Shunmugam M. S.; (2010) A novel method to improve finish on non-magnetic surfaces in magnetorheological abrasive honing process, *Tribology International*, 43:1122-1126.
- Schmitt, C.; Moos, U.; Bahre, D. (2003) Comparison of different approaches to force controlled precision honing of bores. *Journal of Mechanics Engineering and Automation*, 3: 764-771.
- Seok, J.; Kim, Y.J.; Jang, K.I.; Min, B.K.; Lee S. J. (2007) A study on the fabrication of curved surfaces using magnetorheological fluid finishing, *International Journal of Machine Tools & Manufacture*, 47: 2077– 2090.
- Shiou, Fg; Chen, C. H. (2003)Freeform surface finish of plastic injection mold by using ball-burnishing process, *Journal of Materials Processing Technology*, 140: 248–254.
- Shorey, A. B.; Tracy, J. P.; Kordonski, W.I. (2004) Application of Magnetorheological Jet (MR jet) in precision finishing, *ASME International Mechanical Engineering Congress*, 43: 25-39.
- Sidpara, A.; Jain, V.K. (2011) Experimental investigations into forces during magnetorheological fluid based finishing process. *International Journal of Machine Tools and Manufacture*, 51: 358-362.
- Sidpara, A.; Jain, V.K. (2012) Theoretical analysis of forces in magnetorheological fluid based finishing process. *International Journal of Material Sciences*, 56: 50-59.

- Sidpara, A.; Jain, V.K. (2013) Analysis of forces on the free form surface in magnetorheological fluid based finishing process. *International Journal of Machine Tools and Manufacture*, 69: 1-10.
- Singh, A.K.; Jha, S.; Pandey P.M. (2013), Mechanism of material removal in ball end magnetorheological finishing process, *Wear*, 302: 180-1191.
- Singh, D.K.; Jain, V.K.; Raghuram, V. (2004) Parametric study of magnetic abrasive finishing process. *Journal of Materials Processing Technology*, 149: 22-29.
- Stradling, A.W. (1993), The physics of open-gradient dry magnetic separation, *Int. J. Miner. Process* 39: 19–29.
- Wu, X.; Kita, Y.; Koku, K.I (2007) New polishing technology of freeform surface by GC, *Journal of Materials Processing Technology* 188: 81–84.
- Wang, Y.; Hu, D. (2005) Study on the inner surface finishing of tubing by magnetic abrasive finishing. *International Journal of Machine Tools and Manufacture* 45: 43-49.
- Wang, A.C.; Lee, S.J. (2009) Study the characteristics of magnetic finishing with gel abrasive. *International Journal of Machine Tools and Manufactures*, 49: 1063-1069.

Web References

[https://en.wikipedia.org/wiki/Honing_\(metalworking\)#/media/File:WVN_Diam.png](https://en.wikipedia.org/wiki/Honing_(metalworking)#/media/File:WVN_Diam.png)

http://www.columbiagrinding.com/images/lapping_diagram.gif

<http://www.watsongrinding.com/wp-content/uploads/2011/12/Grinding.jpg>